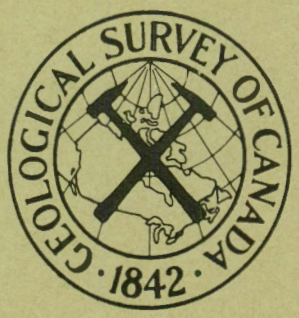

GEOLOGICAL
SURVEY
OF
CANADA

DEPARTMENT OF ENERGY,
MINES AND RESOURCES

PAPER 66-29

SEDIMENTOLOGY OF THE PRINCE GUSTAF ADOLF SEA AREA, DISTRICT OF FRANKLIN

(Report and 17 figures)

J. I. Marlowe

Price, $2.00

1968

GEOLOGICAL SURVEY
OF CANADA

PAPER 66-29

SEDIMENTOLOGY OF THE PRINCE GUSTAF ADOLF SEA AREA, DISTRICT OF FRANKLIN

J. I. Marlowe

DEPARTMENT OF ENERGY, MINES AND RESOURCES

Available by mail from the Queen's Printer, Ottawa,

from Geological Survey of Canada,
601 Booth St., Ottawa,

and at the following Canadian Government bookshops:

HALIFAX
1735 Barrington Street

MONTREAL
Æterna-Vie Building, 1182 St. Catherine St. West

OTTAWA
Daly Building, Corner Mackenzie and Rideau

TORONTO
221 Yonge Street

WINNIPEG
Mall Center Bldg., 499 Portage Avenue

VANCOUVER
657 Granville Street

or through your bookseller

Price $2.00 Catalogue No. M44-66-29

Price subject to change without notice

ROGER DUHAMEL, F.R.S.C.
Queen's Printer and Controller of Stationery
Ottawa, Canada
1968

CONTENTS

Illustrations

Page

ABSTRACT

The Prince Gustaf Adolf Sea area is located on the continental shelf bordering the Arctic Ocean. It is underlain principally by moderately deformed siltstone, sandstone, and shale formations of Mesozoic to Tertiary age that form part of the Sverdrup Basin structural province, and by unconsolidated sand and gravel of the Arctic Coastal Plain (Beaufort Formation). The physical setting is dominated by a polar climatic regime, which maintains an ice cover over the area throughout most of the year.

Physiographic features of the area suggest that the sea bottom has been exposed previously to subaerial processes of erosion. On a broad scale, channels form a dendritic pattern, the gradient of which is generally toward the Arctic Ocean. Smaller scale features suggest that ice action has been effective in shaping the present sea bottom. An island shelf and slope occurs around all the land masses of the area and forms a nickpoint in the bottom profile that may represent a stillstand of sea level 300-400 metres deeper than the present level.

Under present conditions, sand is transported from the islands by ephemeral streams and deposited in relatively shallow depths near shore. Mud covers the greater part of the area. However, sandy layers occur in the sub-bottom at nearshore stations, indicating that hydraulic energy levels at those stations have been higher in the past than they are at present. Sediment textures coarsen with depth in cores from throughout the area and suggest that there was a general lowering of energy levels during the deposition of the sediment contained in core samples. Increasing depth of water associated with a transgressive sea is inferred from these data.

Core samples show that two major stratigraphic units are present in the sediment of Prince Gustaf Adolf Sea. These are (1) an upper, yellow-brown, generally structureless unit containing foraminiferal remains and abundant oxidized, detrital pyrite; and (2) an underlying, grey unit that contains fine bedding structures, fresh, detrital pyrite, and no faunal remains. Contacts between these units are generally transitional, and commonly do not coincide with textural changes. Characteristics of the two units indicate that they were deposited in widely differing sedimentary environments. In the lower unit, the absence of faunal remains and the presence of fresh, detrital pyrite and fine depositional structures suggest a restricted, reducing environment in which there was little or no life. Very fine, cyclical laminae in this unit indicate that glaciers or ice caps may have dominated the sedimentary environment during the deposition of the unit. Beds of the upper unit, however, appear to have been deposited in a relatively well-oxygenated environment in which an abundant microfauna existed. The change from restricted to open, ventilated conditions probably was a result of an incursion of water from the Arctic Ocean over topographic sills into the Prince Gustaf Adolf Sea area. The distribution of foraminifera in the upper unit may be related to former current patterns.

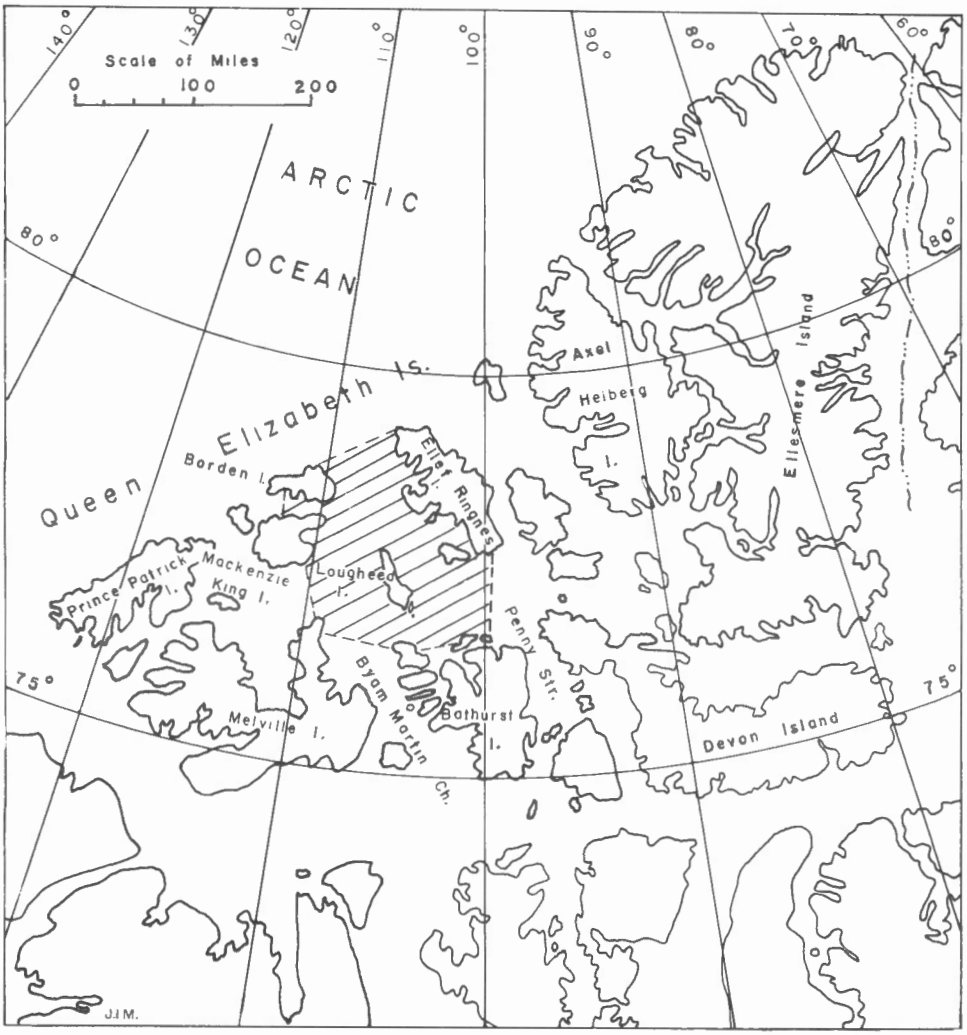

Figure 1. Index map

SEDIMENTOLOGY OF PRINCE GUSTAF ADOLF SEA, DISTRICT OF FRANKLIN

INTRODUCTION

General Statement

Marine geological work in Prince Gustaf Adolf Sea was initiated in the spring of 1962 as part of the Polar Continental Shelf Project of the then Department of Mines and Technical Surveys, and has been carried on since that time by various field parties of the Geological Survey of Canada. These geological investigations were designed to provide a reconnaissance survey of sedimentation on the sea floor as well as detailed coverage of selected near-shore areas. The prime objective of the present study was to define textural and compositional patterns in the bottom sediments and to relate these patterns to past and present oceanographic and geologic factors. The area described in this report includes Prince Gustaf Adolf Sea (Fig. 1), Maclean Strait, and the area south of Ellef Ringnes Island and north of Bathurst Island.

Many of the factors that control sedimentation in Prince Gustaf Adolf Sea are poorly understood. The role of sea ice as an agent of transport and erosion is difficult to assess, and the sedimentary framework is made complex by the effects of tectonic movements of the crust and post-glacial rebound. Only sparse oceanographic information from the study area is available. Although there is little control information other than bottom topography in the area, this study presents a picture of sedimentation on a tectonically active continental shelf in an extreme arctic climatic environment. In an effort to define the sedimentary framework, the compositional and textural data obtained from a detailed examination of 80 bottom sediment samples and cores are presented here.

Location

The area of this report is located in the Queen Elizabeth Islands of the Canadian Arctic Archipelago, between the Sverdrup Islands on the east and Mackenzie King, Borden, and Melville Islands on the west (Fig. 1). It is bounded on the north by the Arctic Ocean and on the south by Bathurst Island and Byam Martin Channel. It includes Prince Gustaf Adolf Sea, part of Wilkins Strait, Desbarats Strait, Maclean Strait, and an unnamed sea area between Ellef Ringnes Island and Bathurst Island.

Associated land masses include Ellef Ringnes, Borden, Mackenzie King, King Christian, and the Findlay Group of islands. The latter include Lougheed Island and four small adjacent islands.

Acknowledgments

Field operations were based on the facilities of the Polar Continental Shelf Project at Isachsen, Ellef Ringnes Island. Logistical support was furnished by E.F. Roots, Coordinator of the Project. The author is especially grateful to Field Supervisors F.P. Duvernet, now deceased, and C. Grant, whose efforts made possible the successful execution of sampling programs in spite of adverse conditions. I. Zemmels, W. Johnson, and J.M.J. Stewart ably assisted in the field work. Special thanks are due to helicopter pilots J. Blake, J-L. Gadet, P. Hort, and H. Easton who, in addition to their flying duties, assisted in handling the sampling equipment. Sounding charts of the area were compiled by hydrographic field parties under the direction of R.M. Eaton, of the Canadian Hydrographic Service. Sediment texture analyses and heavy mineral separations were carried out by R. Cormier, G. Duncan, and S. Pitcher. Much information on the movement of ice in the Prince Gustaf Adolf Sea area was acquired in discussions with Captain J. Cuthbert, of the Department of Transport, and W. Black of the then Geographical Branch, Department of Mines and Technical Surveys.

History of Exploration

The first visit of civilized man to the area of this report was made in the spring of 1901 by Isachsen and Hassel of the Second Norwegian Polar Expedition, under the command of Otto Sverdrup. Departing Cape Southwest at the southern end of Axel Heiberg Island (Fig. 2), Isachsen and Hassel travelled across the ice to the south coasts of Amund Ringnes and Ellef Ringnes Islands, passing northward up Danish Strait along the west coast of Ellef Ringnes Island to Cape Isachsen and taking about six weeks to complete their journey around the two islands (Taylor, 1955, pp. 88-89). Prince Gustaf Adolf Sea, King Christian Island, and a number of associated geographical features were described and named as a result of this journey (Sverdrup, 1904).

The area was next visited by D.B. MacMillan, who, sledging from a base in Greenland, reached King Christian Island in April, 1916 (Taylor, 1955, pp. 99-102). A few days later, he returned eastward across the ice south of Ellef Ringnes Island.

Sledge parties of the Canadian Arctic Expedition, under Vilhjalmur Stefansson, passed through the Prince Gustaf Adolf Sea area at various times

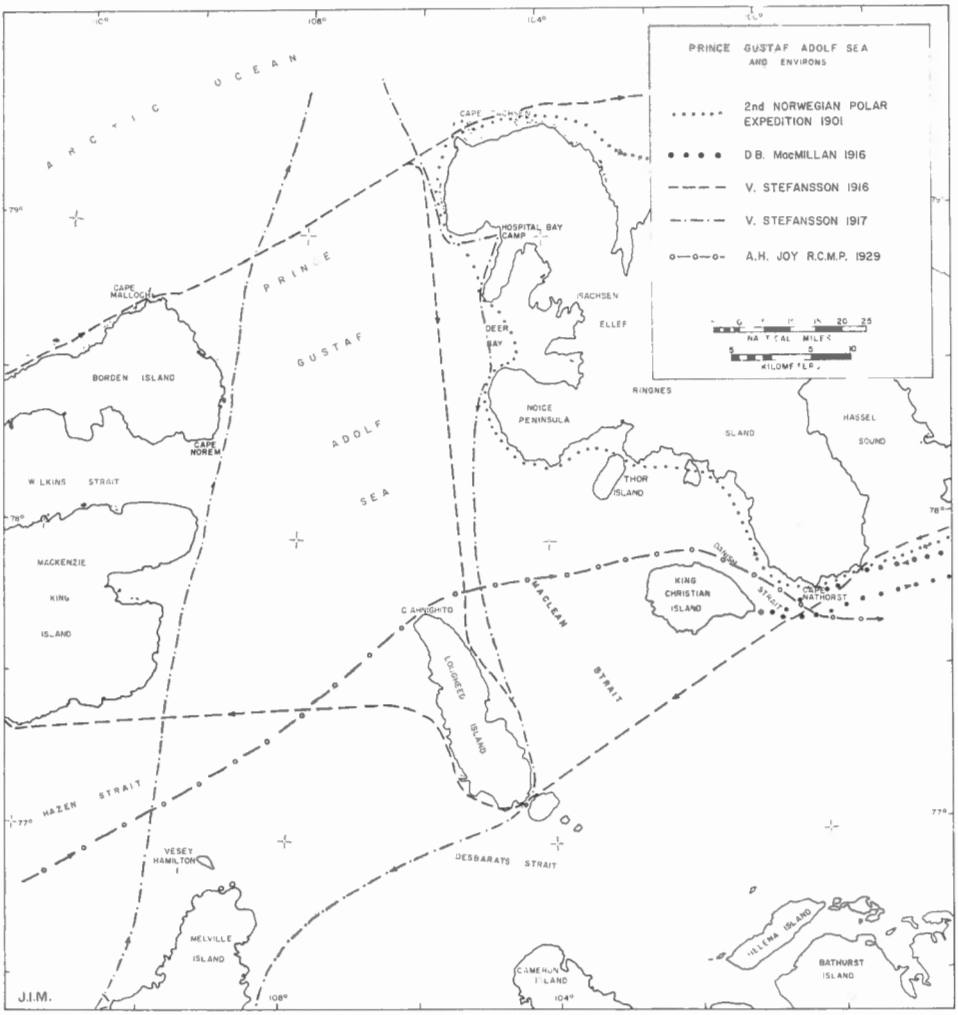

Figure 2. Early exploration routes in the Prince Gustaf Adolf Sea area

during the travel seasons of 1916 and 1917. In May, 1916, a party led by Stefansson sledged northward from Melville Island to Cape Beauchat, on Mackenzie King Island. Stefansson then proceeded northwestward around Brock Island, across Wilkins Strait, and along the north coast of Borden Island. Passing directly across Prince Gustaf Adolf Sea to Cape Isachsen on Ellef Ringnes Island, Stefansson split his party and sent part of it, under Castel, southward towards King Christian Island while he and the remainder of the group continued explorations to the east. After discovering Meighen Island, Stefansson returned westward in June, 1916, touching at the south end of Ellef Ringnes Island, where he found evidence of MacMillan's visit of three months earlier. Continuing his journey to the west, Stefansson and his men landed on Lougheed Island on August 9. Because of poor travelling conditions on the ice, they camped at the south tip of the island until September 3, when the ice was again suitable for men and sledges. The party then travelled up the west coast of Lougheed Island and across Prince Gustaf Adolf Sea to Cape Murray, on Brock Island. Due to the failure of the hunting party under Castel to cache a meat supply at Cape Murray, Stefansson was forced to return to his base on Melville Island immediately. On meeting Castel, Stefansson learned (Stefansson, 1921, p. 563) that he himself was probably not the first to discover Lougheed Island, for Castel's party, on travelling southward down Prince Gustaf Adolf Sea, had touched on the northeast coast of the island. Castel stated that he had erected a cairn on the spot. Although the author's party, during the 1962 and 1963 field seasons, found evidence of Stefansson's visit to the island, no trace of Castel's cairn was located.

Stefansson returned to the Prince Gustaf Adolf Sea area in 1917, en route to the Beaufort Sea. A venture onto the Polar Pack was cut short by an outbreak of scurvy in the party, and the group returned to land, camping for several days at Hospital Bay on Ellef Ringnes Island (Fig. 2).

The route of the 1929 patrol of Staff-Sergeant A.H. Joy, of the R.C.M.P., covered over 1700 miles and crossed Prince Gustaf Adolf Sea from Hazen Strait, around Lougheed Island, and south through Danish Strait.

No further exploration in the Prince Gustaf Adolf Sea area took place until the establishment of the joint Canadian-American weather station at Isachsen, in 1948.

Previous Geological Investigations

Members of the Sverdrup expedition (Sverdrup, 1904) collected geological specimens and commented generally on the physiography of Ellef Ringnes Island. Stefansson (1916) obtained what were probably the first bottom sediment samples from Prince Gustaf Adolf Sea while taking soundings by wire line at scattered locations.

Investigations of the Geological Survey of Canada commenced in the area in 1953 and since that time the regional geological setting has become increasingly well known. Heywood (1957) described the stratigraphy of the Isachsen area, on Ellef Ringnes Island (Operation Franklin). A large-scale investigation supported by aircraft was carried out in 1955 over a wide area of the Canadian Arctic Archipelago, including Ellef Ringnes and parts of Lougheed Islands (Fortier, et al., 1963). As part of Operation Franklin, Roots (1963) described the physiography of Ellef Ringnes Island and the Findlay Group. Gypsum piercement domes and their associated stratigraphy on Ellef Ringnes Island were examined in detail by McLaren(1963), Blackadar (1963), and Greiner (1963). The physiography and geology of part of southern Lougheed Island was described by Glenister and Thorsteinsson (1963).

The geology of the Western Queen Elizabeth Islands, including Borden and Mackenzie King Islands, was described by Tozer and Thorsteinsson (1964) on the basis of field investigations carried out from 1954 to 1959. Papers by the same authors (Tozer, 1960, Thorsteinsson and Tozer, 1960) summarize the structure and stratigraphy of the Canadian Arctic Archipelago on a regional basis.

Marine geological work in Prince Gustaf Adolf Sea and adjacent areas began in 1960, with the support of the Polar Continental Shelf Project (Pelletier, 1962). Since that time, several reports on the bottom sediments and fauna have been made (Wagner, 1962, 1964; Horn, 1963; Marlowe and Vilks, 1963; Vilks, 1964; Marlowe, 1964).

Geological Setting

The Prince Gustaf Adolf Sea area lies within the Sverdrup Basin structural province (Thorsteinsson and Tozer, 1960), a site of sedimentation from Middle Pennsylvanian to early Tertiary time. Sedimentary rocks in this basin lie unconformably on deformed lower Palaeozoic rocks of the Franklin Miogeosyncline (Fig. 3), which are exposed south of the study area.

The axis of the Sverdrup Basin trends northeastward. Beds contained in the basin become thinner toward the northwest and dip southeastward. Deposition in the basin continued through early Tertiary time, after which a period of erosion is presumed to have followed (Tozer, 1960, p. 15). During this time of uplift, it has been postulated (Fortier and Morley, 1956; Pelletier, 1964) that subaerial erosion produced the pattern that is reflected in the topography of the modern islands and channels.

Gypsum piercement domes on Ellef Ringnes Island intrude strata as young as Lower Cretaceous (McLaren, 1963, p. 553), and owe their origin to tectonic movements, which took place during the Tertiary Period (Thorsteinsson and Tozer, 1960, p. 17).

Description of Formations Indicated by Numbers in Figure 3

TERTIARY AND/OR PLEISTOCENE

15- Beaufort Formation - Alluvial and deltaic sand, gravel, and boulders; abundant fossil wood.

CRETACEOUS AND TERTIARY

14- Eureka Sound Formation - Non-marine sand, sandstone, siltstone, and silty shale.

CRETACEOUS

Upper Cretaceous

13- Kanguk Formation - Grey marine shale.

Lower or Upper Cretaceous

12- Hassel Formation - Red and brown, non-marine sandstone and sand.

Lower Cretaceous

11- Christopher Formation - Marine shale, siltstone, and fine-grained sandstone.

10- Isachsen Formation - White, yellow, and brown, non-marine sandstone, grit, and conglomerate; coal; variably lithified.

JURASSIC AND CRETACEOUS

Upper Jurassic and Lower Cretaceous

9- Deer Bay Formation - Black shale; minor sandstone and siltstone; marine.

8- Mould Bay Formation - Grey, greenish grey, and brown marine sandstone and sand; grey shale with calcareous concretions.

JURASSIC

7- Jaeger Formation - Sandstone.

Lower, Middle, and (?)Upper Jurassic

6- Wilkie Point Formation - Grey and green sand, dusky red sandstone; grey phosphatic nodules; on Mackenzie King and Borden Islands, lower part is grey marine shale.

Lower Jurassic

5- Borden Island Formation - Green and red sand and sandstone.

TRIASSIC

Upper Triassic

4- Heiberg Formation - Marine and (?)non-marine, grey and brown sandstone.

3- Schei Point Formation - Marine, grey, calcareous sandstone; limestone; sand.

PENNSYLVANIAN AND/OR PERMIAN

2- Gypsum intrusions, with included limestone and volcanics.

PERMIAN AND OLDER

1- Well lithified rocks of the Franklin Miogeosyncline.

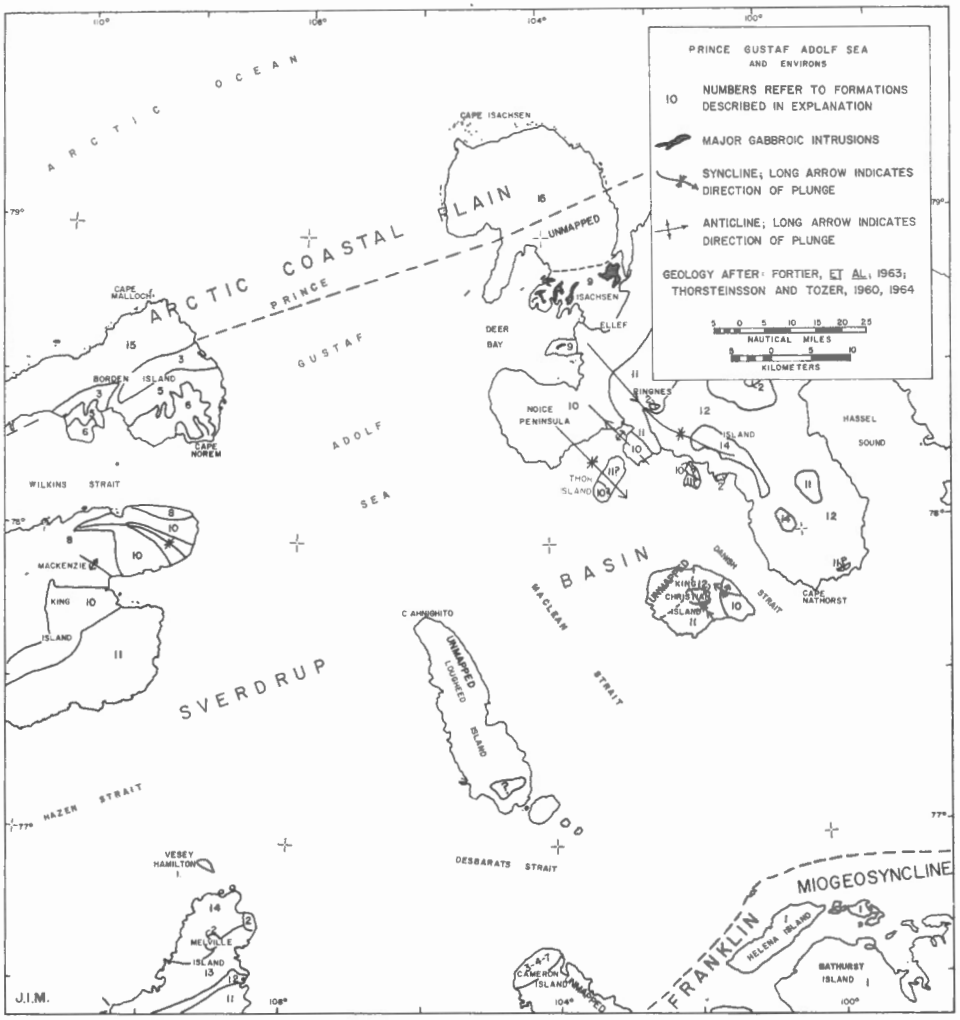

Figure 3. Generalized geology of the Prince Gustaf Adolf Sea area

Rocks of the Sverdrup Basin are bounded on the northwest by sediments of the Arctic Coastal Plain, which underlies a small portion of Prince Gustaf Adolf Sea (Fig. 3). This structural province is composed of late Tertiary or Pleistocene (Thorsteinsson and Tozer, 1960, p. 3) sand of the Beaufort Formation.

Outcropping rocks in the Prince Gustaf Adolf Sea area are mainly Cretaceous to Tertiary in age, although the southeastern half of Borden Island is made up of Triassic and Jurassic formations (Fig. 3; Heywood, 1959; Tozer and Thorsteinsson, 1964, Map 1142-A). The islands are characteristically low-lying and gently sloping toward their shorelines. Local areas of moderate relief occur where sandstone and other resistant formations crop out. In general, the central portions of the islands have greater local relief than the peripheral areas.

Dominant lithologies of outcropping formations in the area of study are sand, sandstone, siltstone, and shale (Tozer and Thorsteinsson, 1964, Map 1142-A). Minor lithologies are represented by diabase bodies, which occur at Deer Bay on Ellef Ringnes Island, and gypsum and limestone from the diapiric intrusions shown in Figure 3. Loose, erratic fragments of exotic lithologies occur in sizes varying up to boulders 3 feet in diameter in the sand of the Beaufort Formation and on the surfaces of other formations. The origin of these erratics has been attributed by Craig and Fyles (1960, p. 2) to ice-rafting during periods of submergence of the archipelago or to transportation in a regional ice-sheet. Glenister and Thorsteinsson (1963, p. 573) suggested that the erratics of Lougheed Island, many of which are striated, owe their origin to ice-rafting. Tozer and Thorsteinsson (1964, pp. 34-36), however, presented evidence that the Beaufort Formation erratics were originally brought into the area by glaciers.

Water and Ice Movements

Little is known of water movements in the area of study. During periods of open water, drift ice has been observed to move southeasterly down Danish and Maclean Straits. The direction of movement of pack ice is generally southward, from the Arctic Ocean down Prince Gustaf Adolf Sea and through Byam Martin Channel and Penny Strait (Fig. 1). Only crude data are available on surface current velocities. In August, 1962, ice was observed to move through Danish Strait in a flat calm at a rate of 10 cm per second (0.2 knot). Oceanographic data by Collin (1961, p. 258) indicate a weak, southwesterly movement of subsurface waters in the vicinity of Ellef Ringnes Island. Prince Gustaf Adolf Sea is covered by ice during most of the year and is open locally only during short periods in the summer. A shore lead, however, develops early in the summer and is commonly wide enough to allow the generation of breakers during periods of strong winds. Ice thicknesses in young ice of the area average about 8 feet during May and June.

Ice is effective both as a beach-shaping agent and in transporting sediment from the shore to sea. The pressure of pack ice upon the shore pushes unconsolidated materials into elongate ridges, which trend parallel to the shoreline. Loose beach materials may become frozen into the shore ice and, when the ice drifts away, removed from the beach. Large accumulations of sand to boulder-size fragments were observed on the ice of Prince Gustaf Adolf Sea at a distance of more than 45 km (25 miles)[1] from shore during the 1962 season; these occurrences provide an indication of the texture and volume of sediment that can be transported away from shore by ice.

Tides measured at Isachsen have a mean range of one foot (Can. Hydrographic Serv., 1965, p. 220). With such a small range of tide, tidal currents are significant only in large bays with restricted inlets, and hence have little effect on the marine sediments of the study area.

Collection of Samples

Bottom samples were collected along lines running between islands and roughly normal to the bottom topography, at intervals of 10 to 15 miles (Fig. 4). This pattern was designed to provide reconnaissance information on the bottom sediments and to bring out major lateral variations in sediment type. In order to study the provenance of locally derived marine sediment, outcrops and major streams on the eastern islands were sampled. Samples were collected during the field seasons of 1962 and 1963.

Operations over the sea ice were carried out by two-man parties in Sikorsky S-55 helicopters. Because of the payload capacity of this aircraft it was necessary to use a light, collapsible sampling rig. During the 1962 season, a Phleger-pattern, gravity corer was used to obtain core samples 3 feet and less in length. This corer was lowered and retrieved through auger holes in the ice by means of a portable, gasoline engine-powered winch. It was not felt that samples collected in this fashion were satisfactory and in the 1963 season a 125-pound piston corer was used in place of the gravity corer. As the piston corer required a larger opening in the ice, field work was delayed until early June, when meltwater holes and cracks had developed to an advanced stage. Poor weather conditions and mechanical failures seriously curtailed sampling operations in 1963 and the sea-bottom program was abandoned when approximately 50 per cent completed. No stream or outcrop samples were obtained from the islands on the west side of Prince Gustaf Adolf Sea.

The locations of sample stations were fixed by a Decca Navigator positioning system. Field sounding sheets furnished by R.M. Eaton, of the Canadian Hydrographic Service, were used as base charts from which the locations of sample stations were selected.

---

[1] Distances are given in equivalent nautical miles.

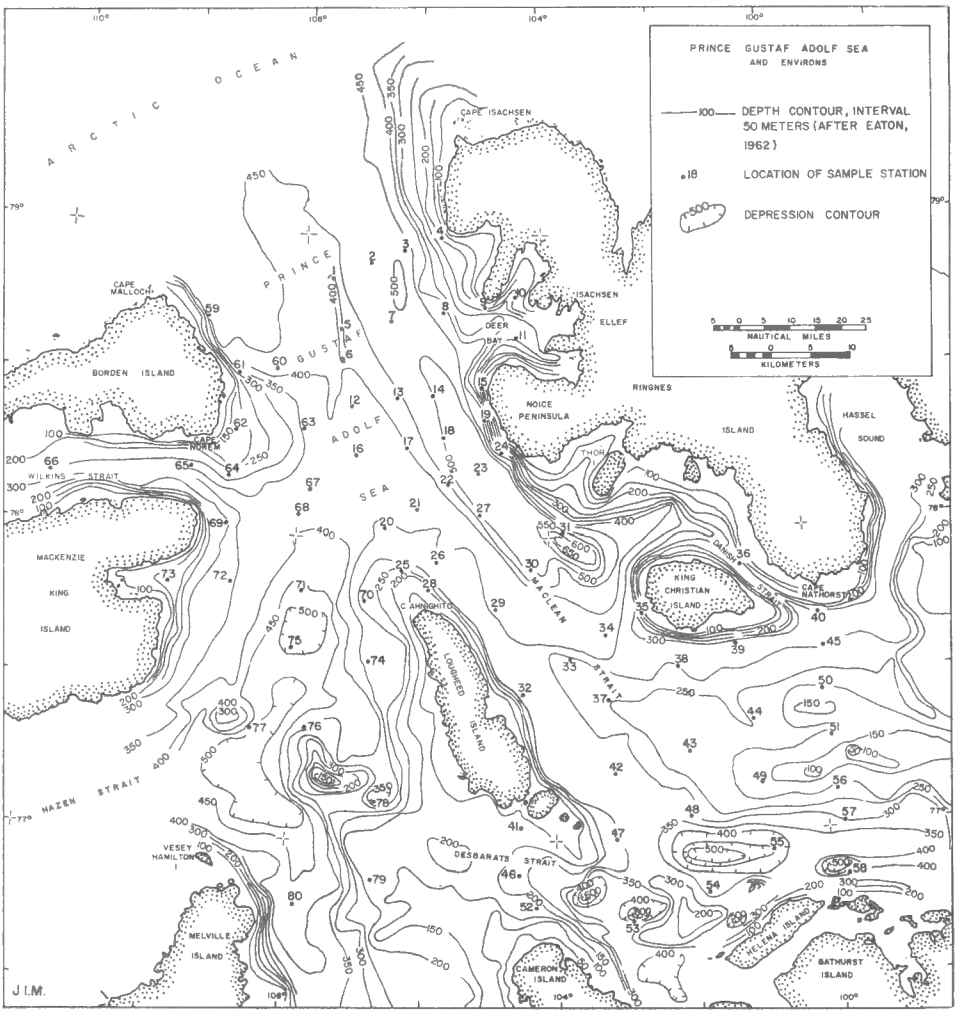

Figure 4. Generalized bottom topography showing locations of sampling stations

BOTTOM TOPOGRAPHY

The submarine topography of the Prince Gustaf Adolf Sea area is characterized by elongated depressions separated by an irregular bottom of moderate depth. Depths increase generally in a northward direction, toward the Arctic Ocean (Fig. 4). Islands of the area rise abruptly from the sea floor and the island shelves surrounding them are distinctive topographic features. Depths over most of the bottom range between 300 and 500 metres. Pelletier (1962, 1964) and Horn (1963) have related submarine topographic patterns in parts of the western Queen Elizabeth Islands to ancient drainage systems. Their conclusions are based upon a hypothesis set forth by Fortier and Morley (1956). Conclusions derived from the present study support conclusions of all the above authors.

Descriptions and interpretations of the submarine topography of the study area are based on sounding charts prepared by the Canadian Hydrographic Service (Eaton, 1962). Depths on these charts were obtained from spot soundings, which are spaced an average distance of 7.5 km (4 nautical miles) apart. No continuous-profile bottom soundings of the area are available, and therefore only major topographic features are defined.

Description of Bottom Topography

For the purposes of this report, the floor of Prince Gustaf Adolf Sea and adjoining marine areas have been separated into physiographic divisions on the basis of contoured bottom soundings (Figs. 4 and 5). These divisions are topographically distinct and were made to facilitate discussion of the area under study. The divisions are named as follows (Fig. 5): Danish Strait Valley; Lougheed Island Ridge; Lougheed Island Basin; Desbarats Trough; Cameron Island Ridge; Berkeley Trough; Grinnell Ridge; and the island shelves and island slopes.

Danish Strait Valley lies off the west coast of Ellef Ringnes Island and extends from King Christian Island to the Arctic Ocean. The valley heads in Danish Strait, between King Christian and Ellef Ringnes Islands. The east side of the valley is formed by the relatively steep shoreface of Ellef Ringnes Island, while its west side is bounded by a sea floor of much lower relief (Fig. 9, Profiles A, B, C, and D). The valley, as defined by the 450-metre contour, is approximately 148 km (80 miles) long and 28 km (15 miles) wide (Fig. 4). The longitudinal profile of the valley is undulating and has low relief (Fig. 6, Profile H). An enclosed basin lies near the head of the valley, where depths of more than 600 metres occur. Tributaries of this valley extend into Deer Bay and between Thor Island and Noice Peninsula (Fig. 4). Horn (1963) described submarine valleys in the channels between Axel Heiberg and Ellef Ringnes Islands (Fig. 1) that exhibit geomorphological features similar to those of Danish Strait Valley.

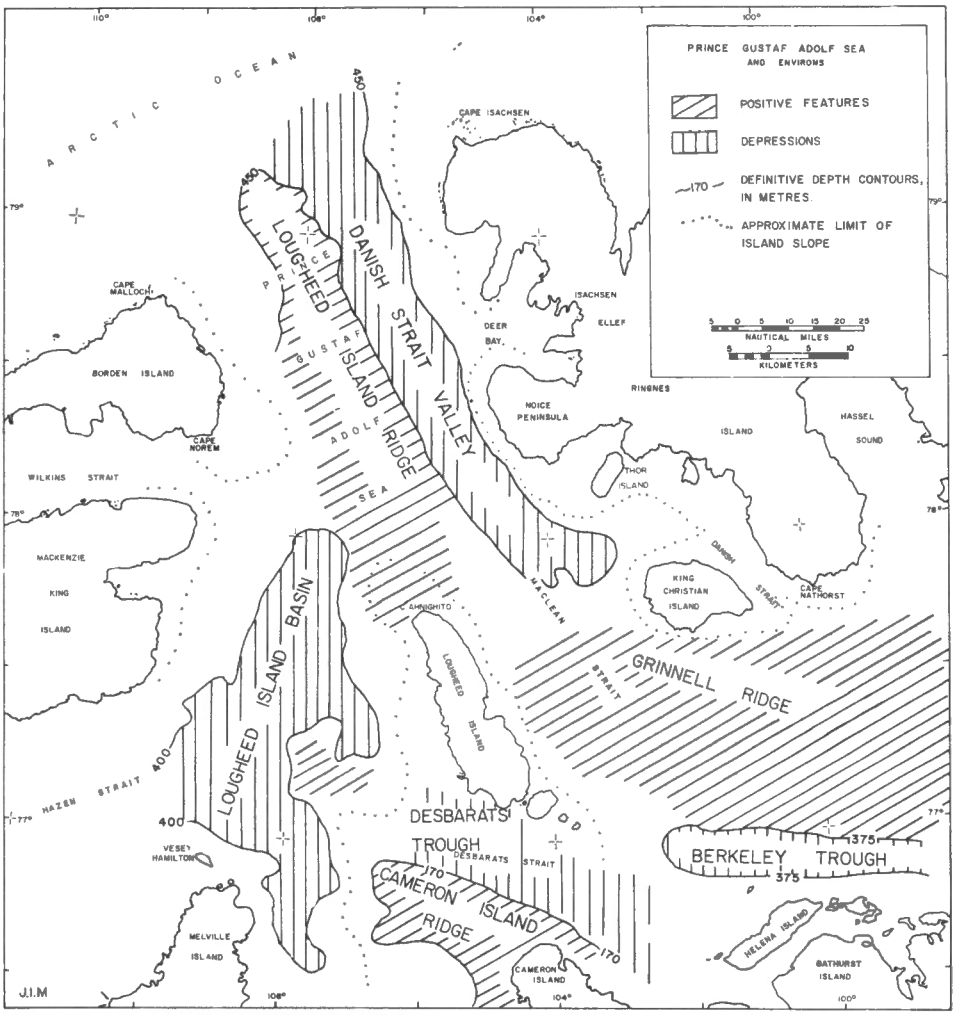

Figure 5. Physiographic divisions in the Prince Gustaf Adolf Sea area

The sea floor west of Danish Strait Valley has low relief and an uneven surface. Lougheed Island Ridge, which has a transverse relief of almost 50 metres at its northern end, lies along the west side of the valley and has a trend that is parallel to that of the valley axis. As defined by the 450-metre contour (Fig. 4), this ridge is approximately 28 km (15 miles) wide. Inside the 400-metre contour, the ridge reflects the shape of the present shoreline of Lougheed Island and has a gradient of 1/100. The bottom between Lougheed Island Ridge and Borden Island appears to be nearly flat off the northeast coast of Borden Island, but depths decrease to the south, giving this area a northerly slope of approximately 1 in 275.

Wilkins Strait, between Borden and Mackenzie King Islands, is straight and has a relatively smooth bottom, which slopes gently eastward into the part of Prince Gustaf Adolf Sea described above. Soundings described by Pelletier (1964, p. 13) show that a topographic sill exists at the western end of Wilkins Strait.

West of Lougheed Island the bottom topography is more complex and consists of a large depression with associated high areas. This depression is referred to in this report as Lougheed Island Basin. The basin, as defined by the 400-metre contour, is elongated in a north/south direction, but is irregular in shape on its east side. It is approximately 35 km (19 miles) wide and 180 km (97 miles) long. A shoal area 20 km (11 miles) by 25 km (13.5 miles) in size occurs at the east side of the basin. This bank is surrounded by deeper bottom on all sides, but is as shallow as 150 metres at its crest (Fig. 4). A depression with a greatest measured depth of more than 500 metres lies adjacent to the southwest side of the bank, resulting in a local relief of 350 metres in 19 km (10.3 miles), or an average gradient of 1/54. A similar, but smaller, positive feature with a crest about 350 metres deep occurs northwest of and across the basin from this bank. The 350-metre contour around the basin extends into the north entrance of Byam Martin Channel. Above 450 m, contours are open at the east end of Hazen Strait; present soundings do not indicate whether the contour lines close upon themselves in that vicinity. A sill with no more than 10 to 15 metres of relief separates the 400-metre contour of the basin from the 400-metre contour 25 km (13.5 miles) to the north of the basin (Fig. 4), and it appears possible that the two contours join off the northeast tip of Mackenzie King Island. The basin does not present, however, the striking linear form of Danish Strait Valley. Rather, it appears to be a closed depression with only limited communication with the Arctic Ocean.

Slopes on the northwest side of Lougheed Island Basin are gentle, averaging 1/200 off East Bay, Mackenzie King Island. Contours in this area (Fig. 4) are smooth and gradients appear to be fairly uniform. Along the east side of the basin gradients are steeper, ranging from 1/200 off Cape Ahnighito to 1/50 at the 150-metre bank. Longitudinal profiles along the floor of the basin reflect uniform, gentle gradients toward the central, 500-metre

contours (Fig. 6, Profile F). Gradients at the mouth of Byam Martin Channel are approximately 1/500 northward; off East Bay, they are 1/500 southward.

In Desbarats Strait, between Lougheed and Cameron Islands (Fig. 4), the bottom topography consists of a broad trough of moderate depth and an associated ridge. These features are here referred to as Desbarats Trough and Cameron Island Ridge, respectively. The trough, as defined by the 170-metre contour, trends roughly north-northeast and is separated from the 200-metre contour around Lougheed Island Basin by a sill having a relief of no more than 15 metres over a distance of 12 km (6.5 miles). A small basin with depths of nearly 300 metres occurs near the middle of the trough and it appears that, with more closely spaced soundings, the 200-metre contour may extend continuously through Desbarats Strait. To the east, depths in the trough increase and exceed 600 metres northeast of Cameron Island. Cameron Island Ridge, defined by the 170-metre contour, is a submarine continuation of the shape of the present shoreline of Cameron Island. It extends from the shoreline to a point 90 km (48.6 miles) northwest, where an abrupt increase in gradient marks the east edge of Lougheed Island Basin. Depths over the axis of the ridge are 200 metres or less. The average gradient down the axis is 1/450.

Berkeley Trough is a large, linear depression with an east-west trend, which lies off the north coasts of the Berkeley Group of islands (Fig. 4). Depths in this feature exceed 500 metres. As defined by the 375-metre contour, it is approximately 100 km (54 miles) long and has an average width of 25 km (13.5 miles). It is situated close to the coasts of the islands to the south of it and the slope of its south side is relatively steep (approximately 1/50). It is bounded on the north by a broad rise and gradients on that side are much gentler. Contour lines at the east end of the trough trend into the north entrance of Penny Strait. Relations between the west end of the Berkeley Trough and the east end of Desbarats Trough are unclear on the basis of sounding information presently available. Widely separated soundings in the 400- to 500-metre range are located off the northwest coast of Helena Island. It therefore appears probable that a large, deep basin exists in that area. This inferred basin does not appear to be directly connected with Berkeley Trough, but is separated from it by a 15 km (8.1 mile) wide sill with a relief of as much as 350 metres. It does appear probable that the basin is a direct continuation of Desbarats Trough, however, on the basis of contour lines shown in Figure 4.

Grinnell Ridge, defined by the 350-metre curve, occupies most of the area bounded on the north by Ellef Ringnes and King Christian Islands and Maclean Strait, on the west by Lougheed Island, and on the south by Bathurst and the Berkeley Group of islands. It is a broad, positive feature with a north-south extent of 65 km (35 miles). It is approximately 100 km (54 miles) long from its western edge to the eastern limit of the present study; soundings to the east of this line indicate that the ridge is a submarine

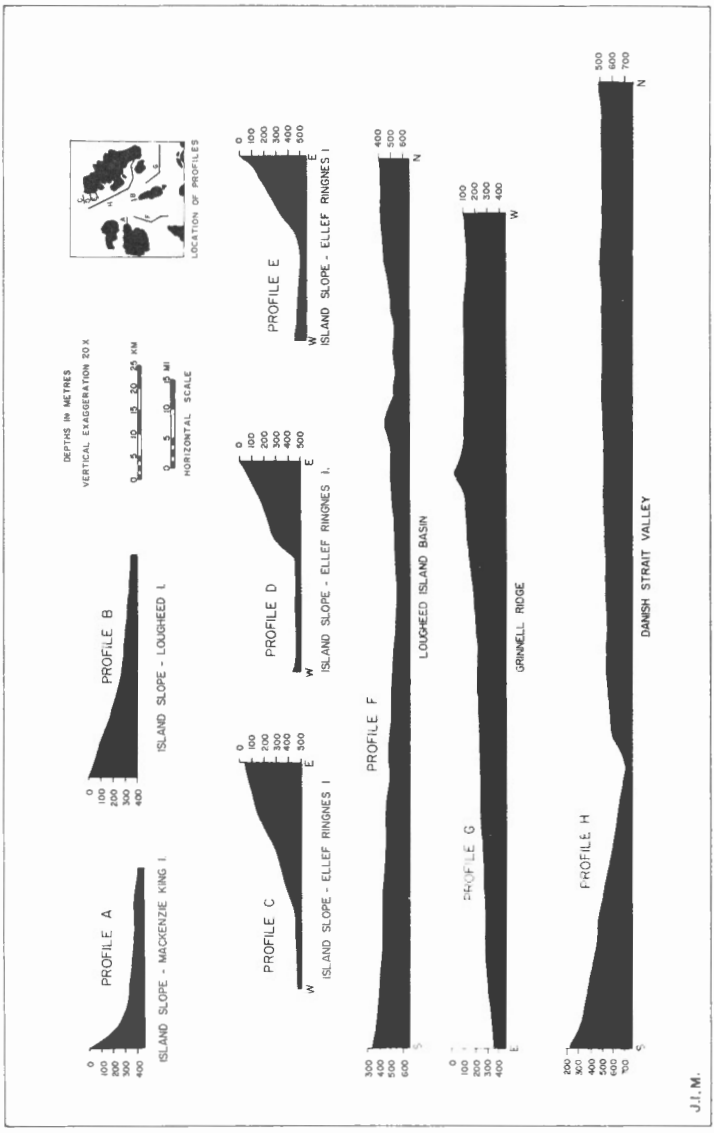

Figure 6. Selected bottom topography profiles

extension of the Grinnell Peninsula of Devon Island. Submarine extensions of Amund Ringnes and Cornwall Islands merge with Grinnell Ridge in that vicinity (Fig. 4; Eaton, 1962). Depths over the crest of Grinnell Ridge are less than 100 metres. Gradients down its north and south flank range from 1/85 to 1/100, being steepest on the south. Gradients down the axis of the ridge, toward the northwest, average 1/800. The longitudinal profile of the ridge is slightly convex (Fig. 6, Profile G).

A characteristic of the bottom adjacent to islands in the study area is a relatively steep slope with a more or less abrupt break at 200 to 300 metres. This slope is referred to in this report as the island slope. Off Noice Peninsula and northeast Borden Island the island slope is 5 to 8 km (2.7 to 4.3 miles) wide and has a maximum gradient of 1/13. Island slopes of similar steepness occur around the east coast of Lougheed Island and the west and south coasts of King Christian Island. Off Cape Norem, Borden Island, the island slope has a gentler gradient, sloping 1 in 80 over a distance of 25 km (13.5 miles). The coast of Ellef Ringnes Island from Deer Bay to Cape Isachsen has a similar island slope (Fig. 6, Profiles C, D, E) with gradients of 1/65 to 1/80 over distances of 18 to 20 km (9.7 to 10.8 miles). Along the east coast of Mackenzie King Island the island slope averages 10 km (5.4 miles) in width and has an average gradient of 1/33. Its profile is concave in its upper portion (Fig. 6, Profile A). The island slope on the west side of Lougheed Island is irregular, varies in its width and gradient, and merges imperceptibly with the upper slopes of Lougheed Island Basin. Southern Lougheed Island has no island slope; instead, the increase in bottom gradient follows along the west side of Cameron Island Ridge.

Interpretation of Bottom Topography

Soundings to the north of the area under study show that the edge of the continental shelf lies nearly 200 km (108 miles) northwest of Prince Gustaf Adolf Sea at a depth of 600 to 700 metres (Eaton, 1962). The study area therefore lies well inside the geological boundary of the North American continent. Water depths over much of the Canadian Arctic Archipelago are greatly in excess of those normally found over continental shelves (Shepard, 1963, pp. 206-261) and, because of this and other lines of evidence, the region is considered to be a drowned continental terrain, which formerly was exposed to subaerial, rather than submarine, processes (Fortier and Morley, 1956; Craig and Fyles, 1960; Pelletier, 1962, 1964).

Fortier and Morley (1956, pp. 7-11) speculated that the present physiographic configuration of the Arctic Archipelago was a result of erosion by a network of rivers that formerly drained a continuous landmass, and related present inter-island channels to ancient stream valleys. Their reconstruction of this subaerial drainage pattern showed, in the Prince Gustaf Adolf Sea area, a dendritic system of streams that flowed from the various high areas in the sea northward to the Arctic Ocean. They further

presented supporting evidence that indicated a Tertiary age for the drainage system. At the time when Fortier and Morley wrote their paper, no soundings in the Prince Gustaf Adolf Sea area were available; it is worthy of note that subsequent data based on recent soundings suggest only minor changes to their inferred drainage pattern.

In an initial report on marine geological activities of the Polar Continental Shelf Project, Pelletier (1962, p. 6) suggested, on the basis of bottom profiles drawn from soundings, that glaciation had modified the shapes of some of the ancient stream valleys postulated by Fortier and Morley. Horn (1963), in discussing the submarine physiography of Peary and Sverdrup Channels, east of Ellef Ringnes Island (Fig. 1), concluded that ice scour has played an important role in the development of bottom topography in that area. From the physiography of the area, he inferred the probable paths followed by glaciers as they moved along the channels to the Arctic Ocean (Horn, 1963, Fig. 1).

Danish Strait Valley in Prince Gustaf Adolf Sea has many of the morphological characteristics that Horn interprets as indicating physiographic modification by glacial action. Its longitudinal profile is undulant; it contains isolated deeps, which may be equivalent to the paternoster lake basins of valley glaciers; and its eastern wall is relatively steep. It appears that Danish Strait Valley may owe its present form to glaciation. Such glaciation must have occurred during a time of lower sea level. Pelletier (1962) pointed out a sharp break in the slope of the bottom at a depth of 400 metres over a submarine ridge north of Cape Isachsen, and inferred that the ridge is a drowned headland. A similar change of gradient at 330 metres occurs on Lougheed Island Ridge, at the lower edge of the island slope. Breaks in slope at the same depth range can be seen at the foot of the island slope around the west coast of King Christian Island and off Cape Norem, Borden Island (Fig. 4). These features are interpreted as drowned shorefaces (Price, 1954, 1955) and are believed to indicate a relative rise in sea level of 300 metres. If the breaks in gradient represent a long stand of an ancient sea level, it can be inferred that much of the bottom of the Prince Gustaf Adolf Sea area was emergent and subject to subaerial erosional processes.

Grinnell Ridge appears to be a submerged, ancient drainage divide. Depths of less than 100 metres in the vicinity of Grinnell Peninsula and Cornwall Island (Eaton, 1962) indicate that the direction of drainage was westward from that area, along the north flank of Grinnell Ridge, and into Danish Strait Valley. Contours on the north side of Grinnell Ridge suggest the presence of northward-trending tributary valleys (Fig. 4). There is no physiographic indication of subsequent glaciation in this area.

Berkeley Trough has morphological characteristics that suggest that glacial scour has influenced its shape. It has an undulant longitudinal profile, and is relatively steep-walled on its south side, and the deep basins along its axis are decidedly elongated. Such features are commonly found in

valleys that have been scoured by glaciers. The most likely direction of movement of glacial ice in Berkeley Trough would be from a source in Penny Strait, where there is an ancient drainage divide (Canadian Hydrographic Service, Chart 7095; Fortier and Morley, 1956, Fig. 3), westward along the trough and then northward, along the east coast of Lougheed Island, to Danish Strait Valley. The west flank of Grinnell Ridge, adjacent to Lougheed Island, does not have the aspect of a glaciated valley. The bottom in this area has a very low relief and there is no continuation of the features in Grinnell Trough that suggest glaciation. As this area is more than 100 km (54 miles) in length, it is to be expected that significant movement of glacial ice along it would result in a more rugged terrain than that described by the contours in Figure 4. If such erosion did occur, it appears that post-glacial modification of the areal topography has taken place.

A second factor that may be significant to the origin of Berkeley Trough is the proximity of the trough to tilted Palaeozoic rocks in the Berkeley Islands, immediately to the south. The contact between Mesozoic and younger rocks of the Sverdrup Basin and the older, more deformed rocks of the Franklin Miogeosyncline lies offshore and somewhere in the vicinity of Berkeley Trough (Fig. 3). Although the regional strike of rocks in the Berkeley Group and Bathurst Island is northeast-southwest (Fortier, et al., 1963, Map 1103A), the possibility of the development of deep basins with an east-west trend as a result of tectonic processes must be considered.

Lougheed Island Basin has on its flanks a complex topography, which suggests subaerial erosion. The isolated bank off the west coast of Lougheed Island rises abruptly from the basinal topography that nearly surrounds it and appears to be a residual highland formed by degradation of the associated low areas. A valley heads on the northeast side of this bank and trends northwestward to the deepest part of the basin. Similar valleys lie along the island slope from Cape Ahnighito to Cameron Island Ridge and off Cape Norem (Fig. 4). These valleys trend into the main axis of the basin and are interpreted as drowned valleys, which were originally formed as subaerial features. There is no clear evidence in these features of erosion by ice; however, it is likely that the basin area did undergo some glacial modification in view of its proximity to the probable glacial valleys around Ellef Ringnes Island.

Desbarats Trough appears to be a low pass in a drainage divide that connects Lougheed Island and Cameron Island. Valley heads on the east and west sides of Cameron Island Ridge indicate that the ridge was a source of drainage at one time. Drainage from the ridge would flow down the island slope on the west and into Lougheed Island Basin, as well as into Desbarats Trough on the north. From Desbarats Trough gradients probably trend both east and west.

SEDIMENTS

General Statement

Sedimentary parameters in Prince Gustaf Adolf Sea suggest that the area has undergone a relative rise in sea level since the deposition of the lowest beds sampled. Bottom sediment is characteristically fine grained and is predominantly clay and clay mud, with sand in excess of 25 per cent occurring only on topographically high areas and near land. There is a general increase of grain size with depth below the bottom, which suggests that current velocities have decreased since the deposition of the lower beds. Sandy lithologies occur farther from shore in sub-bottom samples than they do in bottom samples; similarly, kyanite, which is found only within a short distance of shore in bottom sediments, occurs farther from shore in sub-bottom samples. These characteristics imply a landward migration of a near-shore, sandy facies with a rise of sea level.

Fine-grained sediment is not present on Grinnell Ridge and Cameron Island Ridge, probably because of the scouring action of currents moving over these topographically positive features. Textural and mineralogical data from Grinnell Ridge suggest that parts of this area are closely underlain by bedrock formations that occur on nearby Ellef Ringnes Island. Other mineralogical evidence suggests the occurrence of submarine outcrops elsewhere in the study area.

A dominant feature of the sediments of Prince Gustaf Adolf Sea is a layer of yellow-brown mud which, with a single exception, forms the upper part of all cores studied. The colour of this layer is due to the presence of oxidized iron, most of which occurs in aggregates after pyrite. Unoxidized pyrite is abundant in the beds below the yellow-brown layer. Although the beds underlying the yellow-brown layer are barren of microfauna, the yellow-brown layer itself contains a moderately abundant foraminiferal fauna. This fauna is found in abundance in the open Arctic Ocean and its absence below the yellow-brown layer in cores from Prince Gustaf Adolf Sea implies that circulation of ocean water through Prince Gustaf Adolf Sea did not prevail before the yellow-brown layer was deposited. It follows that the change from a reducing environment, in which pyrite was stable, to an oxidizing environment, in which pyrite is unstable, may have been caused by the incursion of ocean water attendant to a rising sea level.

Methods of Study

Core samples were protected from freezing, where this was possible, and stored in their plastic collecting tubes until brought into the laboratory for study. In the laboratory, the core tubes were split longitudinally and the cores were logged with the aid of a 25X binocular microscope. The

split cores were then wrapped with Saran sheet plastic to prevent drying. One half of each core was preserved and the other was used to provide samples for processing. The upper 4 cm of all cores were sampled and additional, 4-cm long samples were taken wherever the core logs indicated a change in sedimentary conditions. Samples were wet-sieved while still in a plastic state and the sand grains were separated into size classes at whole Phi (ϕ) intervals. Grains of less than 62 microns in size were separated by the pipette method (Twenhofel and Tyler, 1941, pp. 50-55) into whole Phi sizes as small as 9 ϕ.

Sand-size sediments were separated into heavy and light mineralogical fractions by the heavy-liquid method described by Krumbein and Pettijohn (1938, p. 335), using bromoform (sp. g. 2.87) as a medium. Heavy mineral fractions were mounted in Canada balsam and covered; light fractions were mounted on uncovered glass slides for staining. Quartz and feldspars were determined by staining according to methods described by Hayes and Klugman (1959). Heavy abundances were determined by counting all visible grains in successive fields of view until a total of 300 grains for each slide was registered on a laboratory counter. Relative abundances of light minerals were estimated using comparison charts prepared by Shvetsov (Terry and Chilingar, 1955). Mud slides were prepared by allowing mud to settle from suspension onto glass slides; these slides were then studied by means of a high-power petrographic microscope.

Samples for X-ray analysis of mud grains were prepared by sedimentation on glass slides. All X-ray samples were subjected to Cu K α radiation in a Philips Model 12045 diffraction unit with a 1° aperture. Each sample was bombarded through an angle of 60° at a rate of 1°2θ per minute.

Snapper samples and scoop samples were split in a Jones sample splitter and separated into textural and compositional fractions according to standard sedimentological procedures. All samples, with the exception of those that were dry when collected, were wet-sieved. Thin-section mounts were made from well lithified bedrock samples for study with the petrographic microscope.

Texture and Structure

Bottom sediments in the Prince Gustaf Adolf Sea area are mud, sand, and mixtures of mud and sand. Small quantities of pebbles are scattered as isolated grains throughout the finer materials. The general distribution of bottom sediment textural types is shown in Figure 7, in which mud-size sediment has been arbitrarily classified according to its silt and clay content into mud, clay mud, and clay. These subclassifications are intended to bring out fine variations in predominant textural types. It is evident in Figure 7 that the greater part of the study area is covered with clay and clay mud. There is in general an inverse relationship between depth of water and grain size.

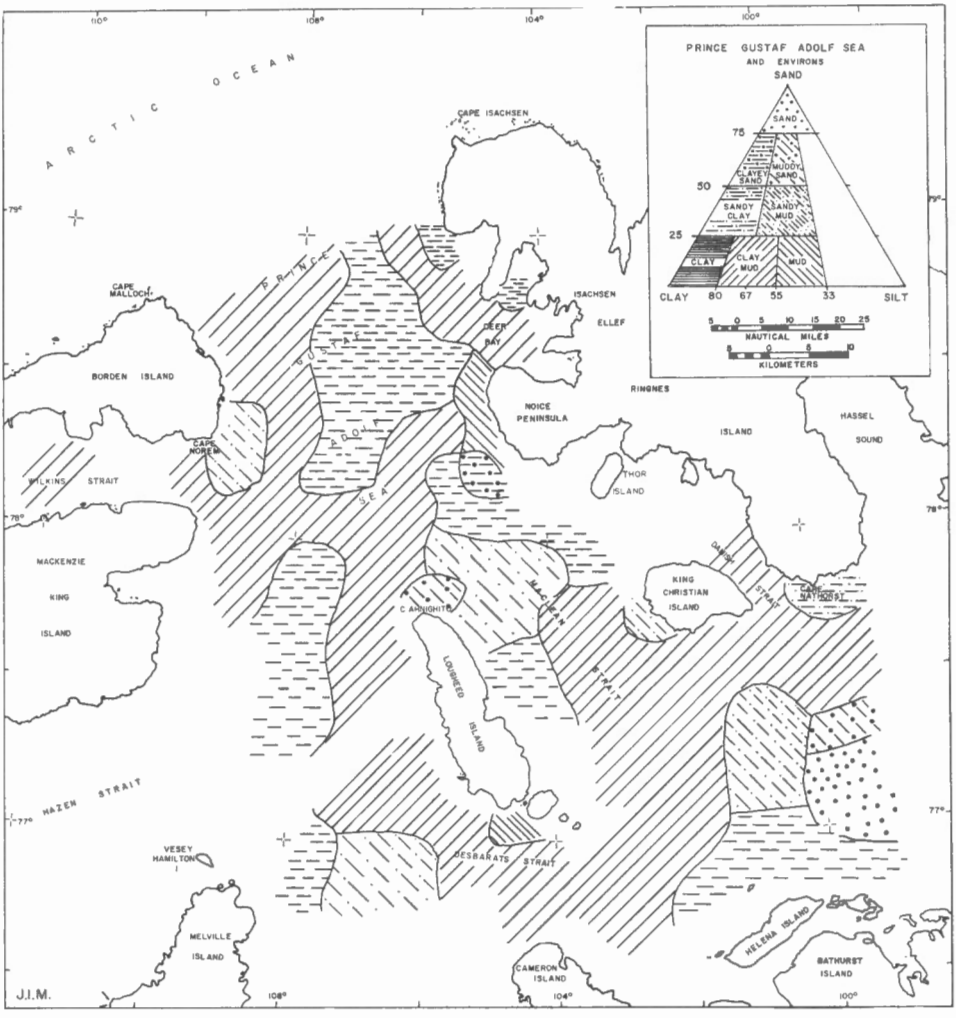

Figure 7. Bottom lithofacies

Sand in small proportions occurs mixed with the finer-grained sediments in the relatively shallow zones around islands and on the island slope of Cameron Island Ridge and sand is the predominant textural class on the crest of Grinnell Ridge. Large areas of clay occupy the deeper parts of Lougheed Island Basin, Berkeley Trough, and Danish Strait Valley; however, an equally large area of clay lies across Danish Strait Valley and Lougheed Island Ridge in the northern part of Prince Gustaf Adolf Sea, with no apparent relationship to topography.

Sediment is coarsest over Grinnell Ridge and off Cape Ahnighito and, in both of these cases, there is a gradual increase in mud content toward greater depths. In Figure 7, the greatest depths of the area contain the finest-grained textural types. Textural classes of intermediate grain sizes occupy intermediate depths of low relief. Although there is a general relationship between distance from land and grain size, which more or less concurs with the relationship between depth of water and grain size already discussed, it can be seen from a contoured plot of median grain sizes (Fig. 8) that major exceptions to this generality exist. Sandy sediment on Cameron Island Ridge occurs at a distance of 55 km (30 miles) from land; similarly, sand on Grinnell Ridge occurs in the centre of a sea area. Both of these lithotopes are located on topographic highs and there can be little doubt in these cases that grain size is more closely related to topography than to distance from shore.

Textural characteristics are plotted against bottom profiles in Figures 9 and 10. In nearly all of these profiles, there is a gradual decrease of grain size toward deeper water. Profiles HH' and II' (Fig. 10) are drawn across Grinnell Ridge and show clearly how the proportional contents of silt and clay increase with depth of water over the ridge. Profiles AA' and EE' (Fig. 9), drawn between Noice Peninsula and Cape Norem and along the axis of Lougheed Island Ridge, respectively, also show an increase in clay content at the expense of sand with increasing water depth. Grain size analyses from individual samples on these profiles (Fig. 11) show that there is in general a decrease in median size of silt with increasing depth, as well as a decrease in relative abundance of the coarser silt grades. The relative abundance of clay and finer silt grades increases with depth of water. It is an accepted sedimentological working hypothesis that sediment texture reflects the energy level of the depositing medium, and that there is in general a direct relation between size of grain in a sediment and current velocity in a sedimentary environment (e.g. Hjulstrom, 1938; Pettijohn, 1957, pp. 588-598). It therefore can be said that most bottom samples in the Prince Gustaf Adolf Sea area indicate that sediment on topographically high areas represents an environment of higher energy level than does sediment in relatively low areas. A notable exception to this generalization is Sample 23 (Fig. 4), in Danish Strait Valley off Noice Peninsula, which contains 53 per cent sand.

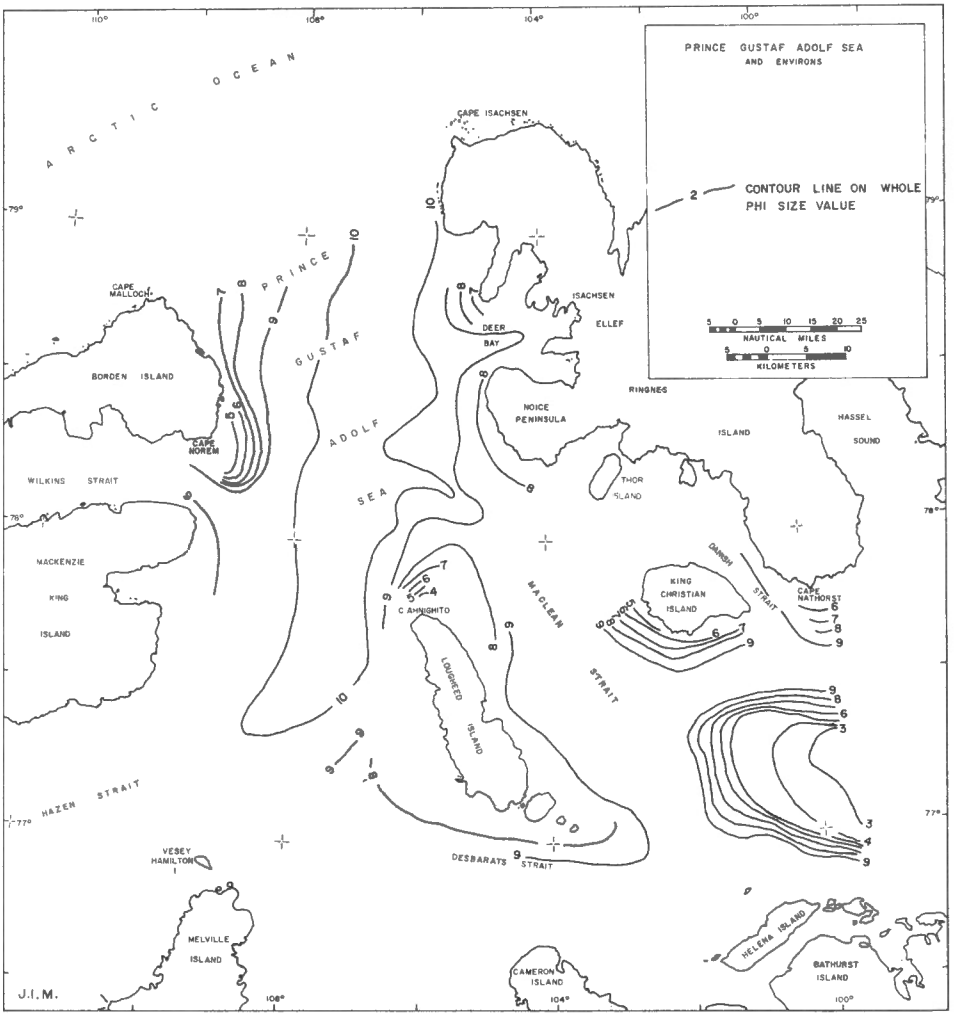

Figure 8. Median grain size of samples from upper 4 cm of cores

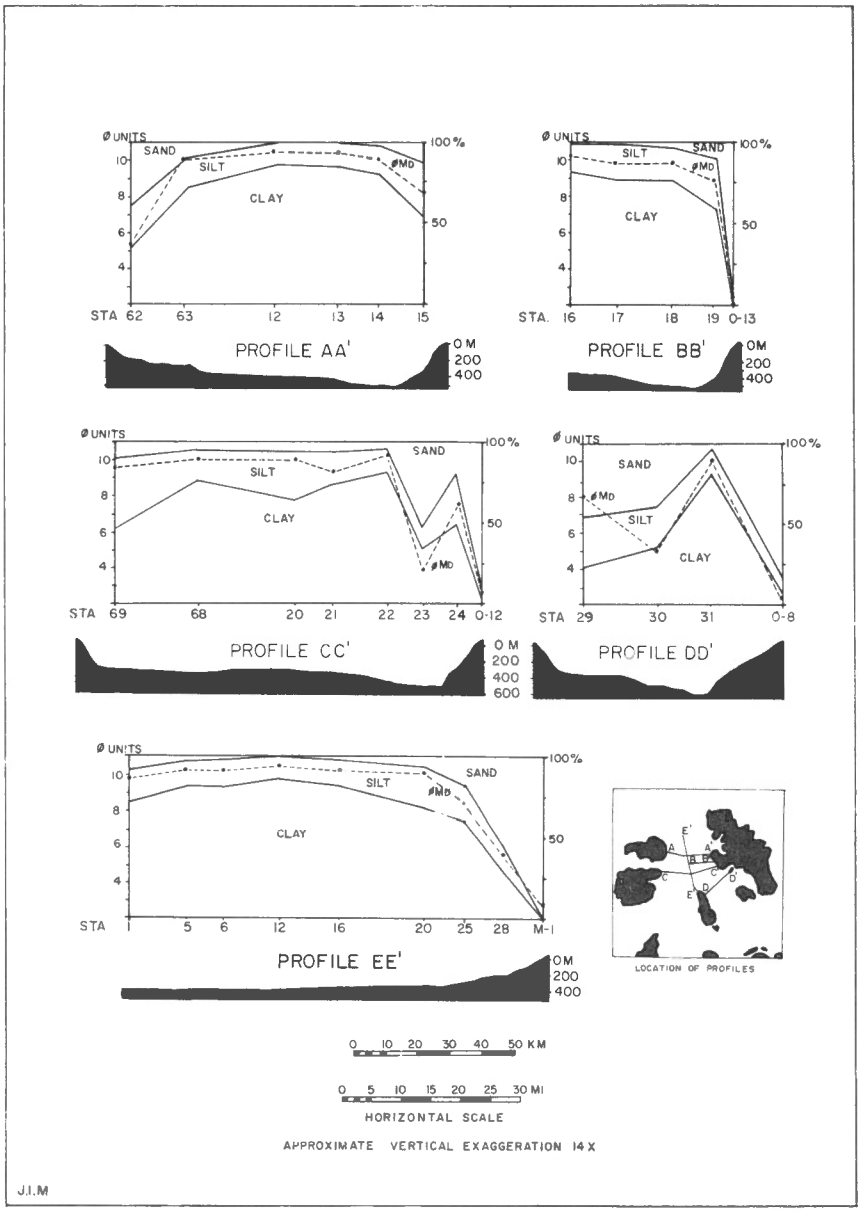

Figure 9. Variation of bottom sediment texture with water depth

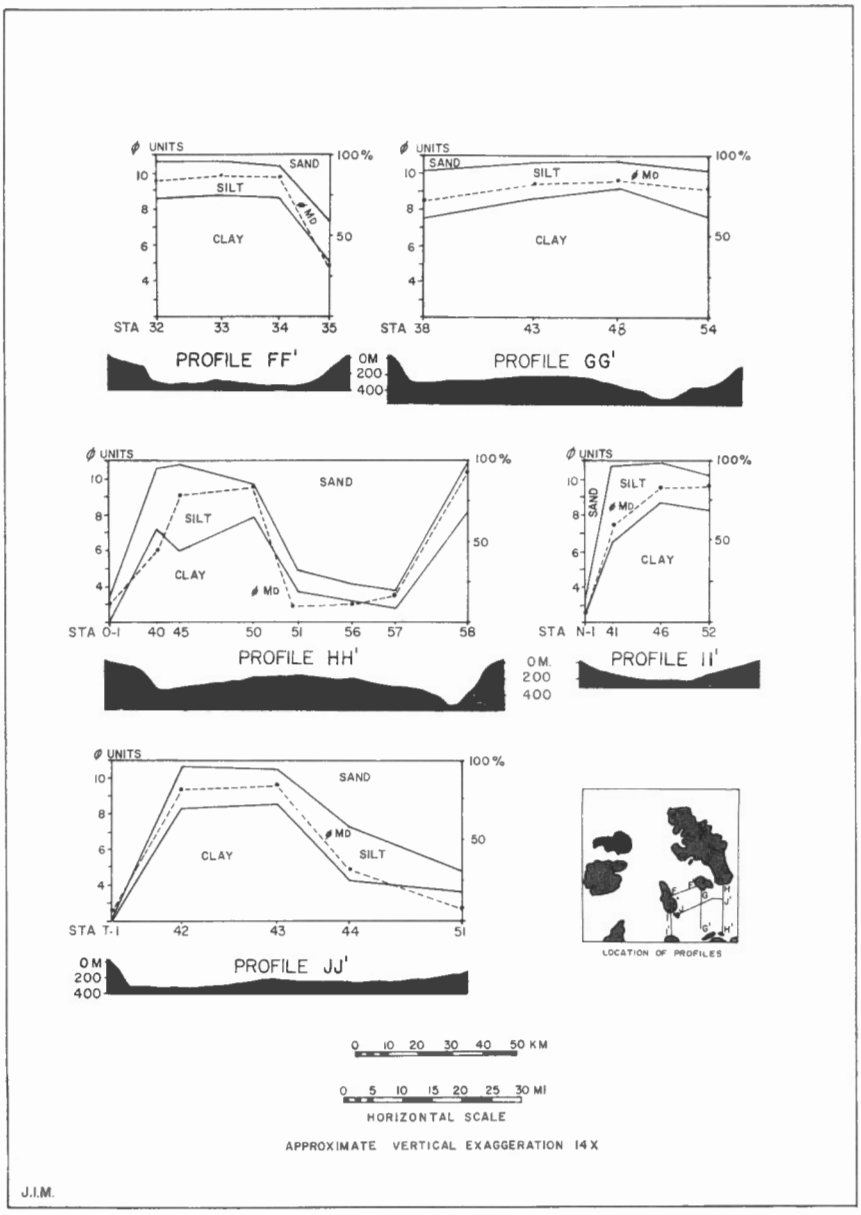

Figure 10. Variation of bottom sediment texture with water depth

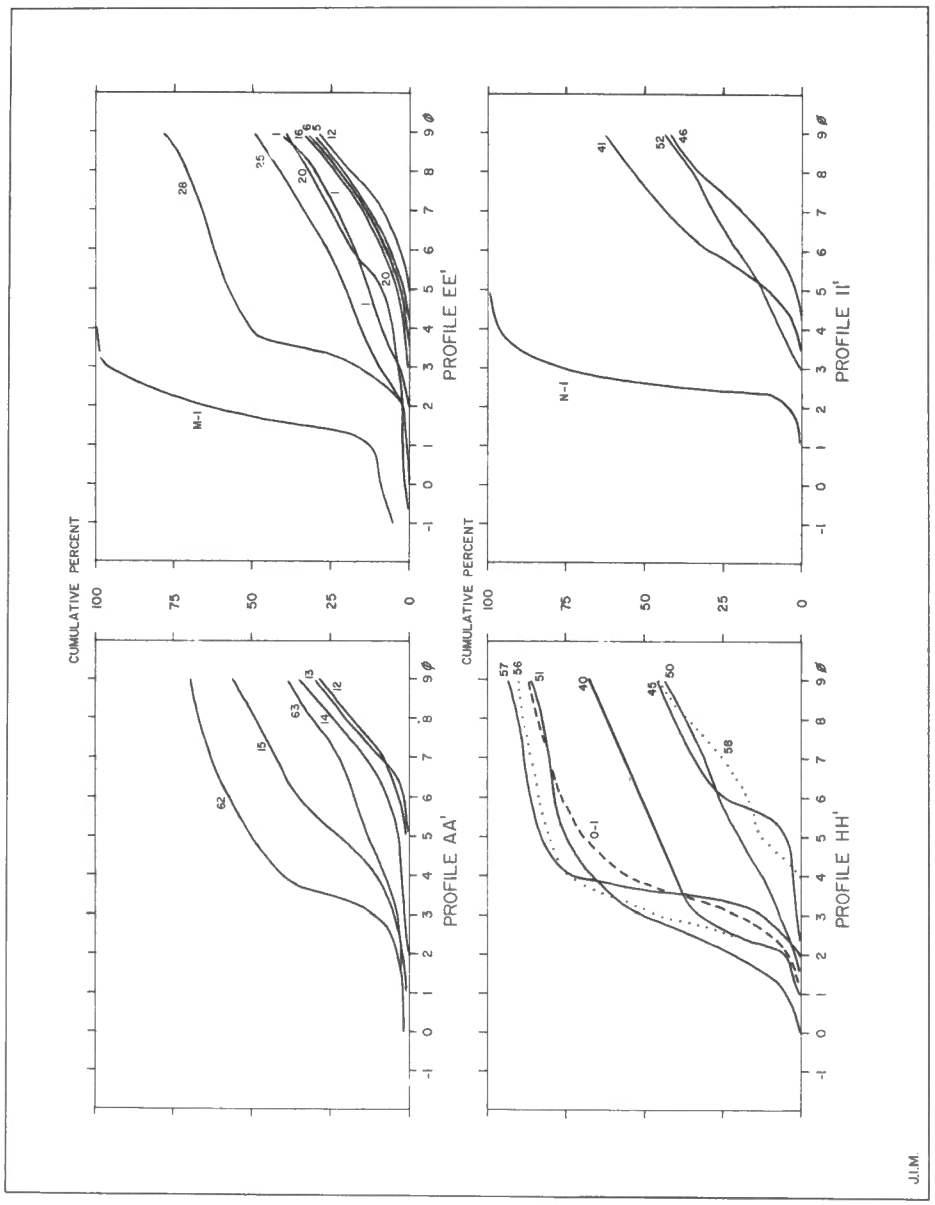

Figure 11. Grain size distribution curves from samples on selected profiles from Figures 9 and 10

Owing to the high percentages of clay-size grains in the sediments of the area of study, it is not feasible to present a complete statistical description of sediment textural parameters. Pipette analyses were carried out to give standard grain size class percentages by weight to 9 ϕ, or the coarse clay class. Grains smaller than 8ϕ are therefore considered as the total clay-size fraction. Sorting values cannot be computed for most of the samples, as size-distribution curves do not extend as far as one Phi standard deviation interval smaller than the median, or even as far as the 75 percentile, for most samples. It was necessary to extrapolate curves in some instances to provide median grain size values. Textural data as presented in Appendix B are therefore given as weight per cent contents of sand, silt, and clay, Phi median diameter (ϕ Md), and ϕp16 (the grain size at one standard deviation interval larger than the median). The latter parameter is included to provide some indication of sorting as shown by distributions at the coarse end of the size scale. Graphic standard deviation values $\frac{(\phi p84 - \phi p16)}{2}$ are given for those few samples on which ϕp84 measurements are available.

Oxidized Sediments

With one exception (Core 36, from Danish Strait), the upper parts of all cores taken in the area of study are composed of sediment of various shades of yellowish brown. The contrast in colour between these upper portions and the medium-to-dark grey sediments underlying them is the most apparent characteristic of the cores described in this study. Similar yellow- to red-brown veneers on sea-bottom sediments in northern latitudes are reported by Horn (1963, p. 8), Leslie (1963, p. 11), and Belov and Lapina (1958). Contacts between the two colour zones are sharp, although interlaminations of sediment of both colours can generally be detected. Bedding in the yellow-brown, near-surface layer is rare and is generally seen only as laminations in the lower few centimetres. Also characteristic of the yellow-brown layer is the presence of a moderately abundant benthonic faunal assemblage. This faunal assemblage is totally absent in the darker-coloured, underlying layers, in which bedding structures are common. This association suggests that the lower beds were deposited in an environment that did not support an abundant benthonic fauna and that such a fauna was present during the deposition of the upper, yellow-brown beds. Burrowing and feeding activity on the part of the fauna probably is responsible for the homogeneous nature of the upper layer.

The colour transition described above is widespread over the entire study area and is considered to be indicative of a major change in sedimentary conditions. Evidence from two cores (63 and 71, see Appendix A) shows that, while darker-coloured sediment was being deposited at some localities, light-coloured sediment was being deposited elsewhere. Yellow-brown clay pebbles in a dark grey matrix occur in Core 63, and a 22 cm-thick, brown sand bed is overlain and underlain by grey mud in Core 71. Although contacts between the two colour types are sharp in gross aspect in

most cores, fine interlaminations of dark grey and yellow-brown mud in the contact zone indicate that conditions responsible for the colour change were related to source or environment of deposition, and not to post-depositional processes. The yellow-brown colour of mud in these sediments is considered to be due to the presence of oxidized iron minerals. Evidence to support this statement is presented later in this report. The yellow-brown layer therefore is probably the product of an oxidizing environment.

Thickness of the upper, yellow-brown sediment layer ranges between 6 and 54 cm over the study area (Fig. 12). Thickness appears to have little relation to either bottom topography or sediment texture (Figs. 4 and 7). Some areas of accumulation in excess of 15 cm are located close to islands (e.g. in Fig. 12, the areas off Cape Norem and Deer Bay) and therefore may be related to sediment sources on land. Similar and greater thicknesses, however, occur in Lougheed Island Basin and in eastern Desbarats Strait. Areas of least thickness lie along the southwest side of Danish Strait Valley and the east side of Lougheed Island, across part of Grinnell Ridge, and at the north end of the sea between Borden Island and Ellef Ringnes Island.

It is not feasible to relate the variation in thickness of the yellow-brown layer to rate of sediment accumulation, as there is no means of age correlation between contacts in different cores. However, the thickness of the layer can be considered as an index of the relative effectiveness of the oxidizing environment in which the sediment comprising the layer was probably formed. The thickness of the layer at a given point is the result of interacting factors of sediment supply, nearness to source, and the hydraulic conditions at the site of deposition. The net accumulation, however, reflects the total effectiveness of the oxidizing environment at that point. Figure 12 indicates that the oxidizing environment has been less effective in the eastern half of the study area than it has in the western half. Eastern Desbarats Strait, however, has the greatest thickness of the yellow-brown layer. The full significance of the pattern in Figure 12 is not apparent at this time. However, it is postulated that, as effectiveness of oxidation is apparently not related to any single sedimentary parameter, the pattern reflects amount of sediment accumulation modified by oceanographic factors. It appears possible that oxidizing conditions have prevailed in western Prince Gustaf Adolf Sea for a longer period of time than they have in the eastern part of the area. Thickness variations in the Berkeley Trough-Desbarats Strait area suggest that oxygenation, and hence water movement, has been more effective in the vicinity of Byam Martin Channel than it has in the vicinity of Penny Strait.

Layers of iron oxide-stained sediment occur in several cores. These layers are coloured in shades of orange-brown and are considered to owe their colour to the presence of abundant limonitic minerals. These minerals are very fine grained and generally occur as coatings on sand grains. Sediments containing such minerals reflect the influence of strongly oxidizing

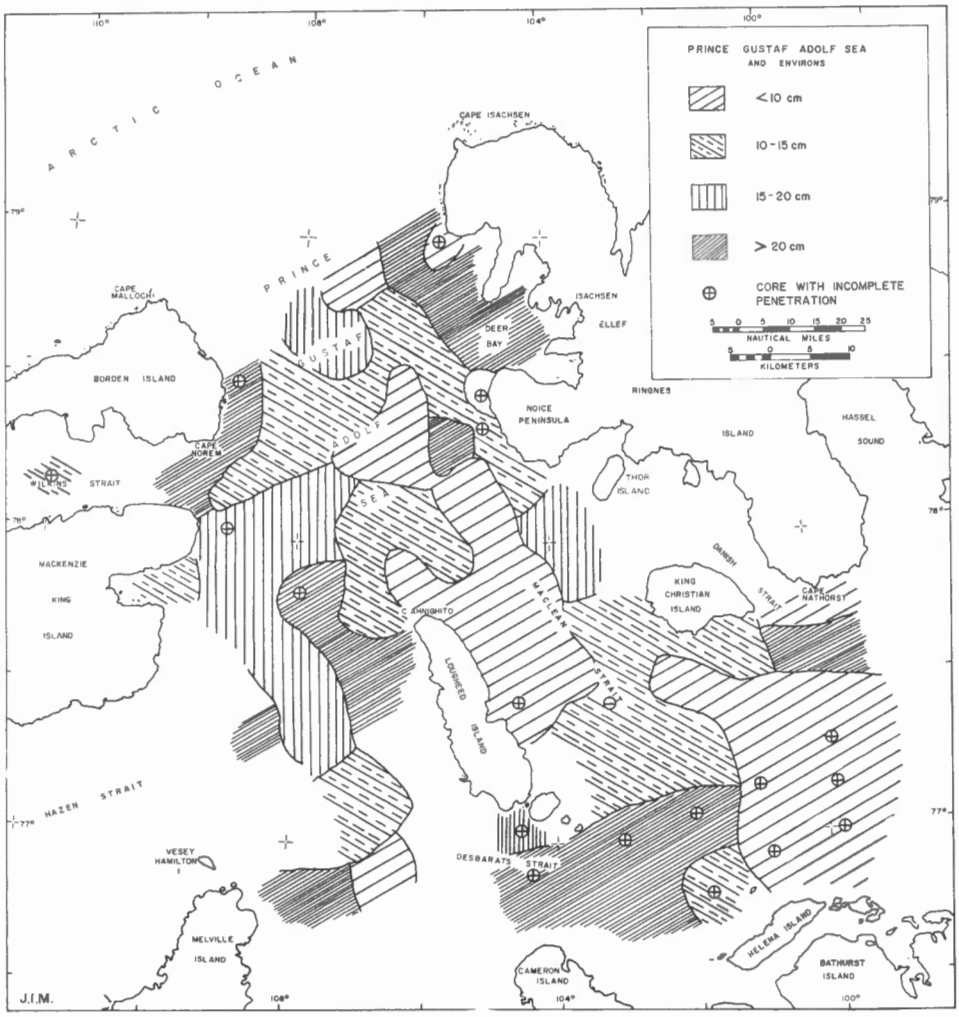

Figure 12. Thickness of yellow-brown layer of sediment

conditions. Core 10, from a depth of 214 metres in Deer Bay, contains a 3 cm-thick layer of iron oxide-stained sand at 20 cm below the present bottom (Appendix A). Core 73, from a depth of 186 metres in East Bay, has a 3 cm-thick layer of laminated, iron oxide-stained mud at 10 cm. Both of these cores are from localities that would be influenced by subaerial weathering during a stand of sea level 180 to 200 metres lower than present sea level; even if they did not actually become emergent, it is probable that these areas would receive subaerially oxidized sediments from enclosing, shallower areas. Core 62, from a depth of 151 metres off Cape Norem, contains a 1 cm-thick layer of muddy sand, which is heavily stained by iron oxide (Appendix A). Fibrous casts in the limonitic matrix resemble the fragments of mossy plants that are commonly found in very shallow water off the present coasts of the area. Horn (1963, p. 9) reported reddish yellow oxidized layers containing plant remains from depths of less than 190 metres in the Peary Channel area. He described these layers as soils and inferred that the stations from which they were collected were formerly exposed to subaerial weathering conditions. No soil layers were observed in the cores from the Prince Gustaf Adolf Sea area; however, the iron-stained deposits described above occur in depths similar to those described by Horn and may be a result of sedimentation in a very near-shore, if not subaerial, environment.

Cores 65 and 68 were taken in depths of more than 300 metres from stations in Wilkins Strait and 35 km (19 miles) east of Wilkins Strait, respectively. Both of these cores contain layers of moderately well sorted sand with limonitic grain coatings at the base of the upper, yellow-brown, mud layer. Core 34, from 362 metres in Maclean Strait, contains a 1 cm-thick layer of iron oxide-stained muddy sand at the top of a bed of grey, muddy sand (Appendix A). Grain packing fabrics in all three of these sand layers suggest sorting and deposition by water currents. The zonal nature of the oxidized layer in Core 34, in particular, indicates that it is the oxidized top of a muddy sand bed, which was deposited in its entirety under fairly constant hydraulic conditions. It appears that either deposition from a nearby subaerial sediment source or erosion in a subaerial environment is responsible for the oxidized layer at the top of this bed.

Beds Below the Oxidized Layer

Below the yellow-brown layer there is a general trend to coarser lithologies. These textural changes do not generally coincide with the change in colour to shades of grey (Fig. 13), although in some cores (e.g. Cores 30, 32, 46, 64, and 76) lithologic zone contacts and colour zone contacts occur on the same horizon. Correlation between beds below the present sea bottom is not feasible on the basis of the evidence presented here. Cores from over the entire area of study, however, contain textural variations that indicate a general lowering of hydraulic energy levels with time. Energy levels now are lower than they have been since the deposition of the deepest beds sampled in nearly all cores, regardless of the topographic location of

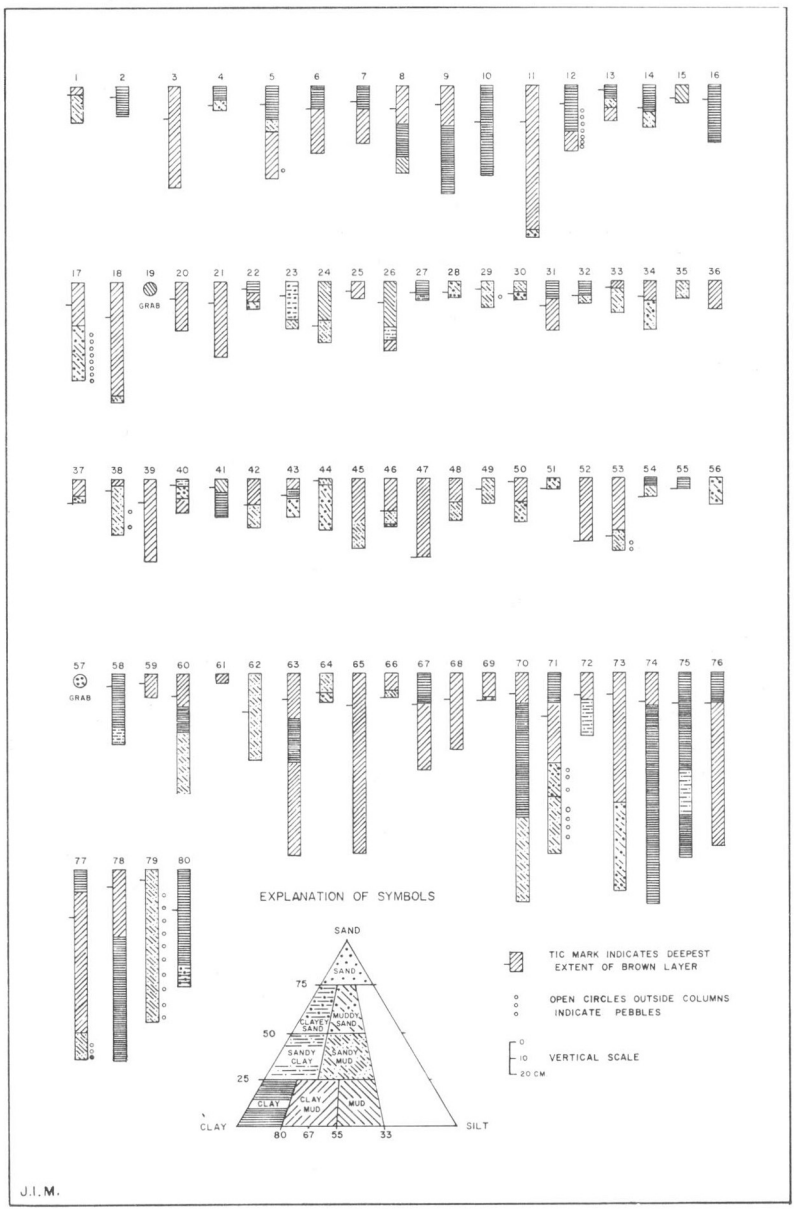

Figure 13. Graphic logs of sediment cores

the cores. Such a change in energy level is compatible with the idea of steadily increasing water depth, which was discussed previously in this report (p. 11). Seven cores have slightly coarser lithologies at their tops than they do at lower levels. These are Cores 8, 9, and 41, which are located near shore, Core 43, from Grinnell Ridge, and Cores 70, 74, and 78, from the east side of Lougheed Island Basin (Fig. 4).

Bedding structures are common in the beds below the yellow-brown layer and are present as laminations in many cores. Cores 52 and 78 (Appendix A) contain 1 to 4 cm-thick, interbedded layers of brown and grey sediment. Cores 18, 65, 74, 76, 77, 78, and 80 contain cyclic laminae of colour-banded clay mud and clay (Fig. 13) in their lower parts. This type of bedding is most marked in cores from Lougheed Island Basin (Cores 74, 76, 77, 78, and 80). Nearly 1.5 metres of cyclical sedimentation is recorded in Core 74 (Appendix A), in which individual cycles range from 2 mm to 2 cm in thickness. The most common sequence is a gradual upward transition from dark grey to light grey mud, followed by a sharply defined contact with the base of the next dark mud bed. There is no clear relation of colour to texture in the cycle. In Core 76, the darker layers are slightly coarser than the lighter layers (as determined by binocular microscopic examination), while there is no apparent size variation between layers in other cores containing the cyclical beds. These beds are similar in their cyclical aspect to seasonally deposited, glacial lake varves and it is suggested that they had a similar origin. The topography of Lougheed Island Basin is such that it would be partly restricted from the open ocean at a lower stand of sea level. If sea level were lowered as much as 300 metres, as it has been suggested elsewhere (Pelletier, 1962; Horn, 1963), the basin area would contain a large water body with only limited communication with the Arctic Ocean. Evidence presented by Craig and Fyles (1960, p. 1) and Pelletier (1964) points to the former existence of ice caps over the western Queen Elizabeth Islands. Seasonal deposition from an ice-dominated, terrestrial sediment source into a restricted water body with poor circulation could produce rhythmically banded sediment of the type cored from Lougheed Island Basin. Cyclical laminae in Cores 18 and 65 are extremely fine (1-5 mm thick) and no textural variation between layers is evident. Both of the latter cores are located near land and in open topography, and it is suggested that their finer structure is a result of relatively slower sedimentation than that of Lougheed Island Basin.

Pebbles and Consolidated Sediment

Ten cores from the area contain significant amounts of pebbles. Four of the cores are located on Lougheed Island Ridge (Cores 5, 12, 17, and 20, Fig. 4); two are on the north edge of Grinnell Ridge (Cores 29 and 38, Fig. 4); and one is on Cameron Island Ridge(Core 79, Fig. 4). Two of the remaining three cores are in Lougheed Island Basin (Cores 71 and 77, Fig. 4) and one is in Desbarats Trough. The locations of cores containing pebbles over Lougheed Island Ridge suggest that this feature has been subjected to

higher energy conditions in the past. Similarly, traces of gravel around the flanks of Grinnell Ridge and Cameron Island Ridge imply higher energy levels in those areas. Although sorting is poor in all the above samples, well-imbricated grain fabrics indicate that most of the sandy, pebbly mud beds are water-laid and are not ice deposits. These beds probably represent conditions of sedimentation at a time of lower sea level, when the topographic highs in question were influenced by processes characteristic of shallow water. The pebbles in Cores 5 and 12, at the northern end of Lougheed Island Ridge, occur in otherwise fine-grained beds and may have been transported by ice rafting. Cores 71 and 77, in Lougheed Island Basin, contain pebbly, sandy mud in beds with random internal structures. These beds may be tills or poorly-reworked glacial-marine deposits.

Pebbles in trace amounts occur in nearly all cores and are scattered randomly throughout other lithologies. These occurrences are considered to be the results of ice-rafting (transportation by floating ice). There is ample evidence from field observations that this process is effective in the area of study (p. 8 , this report). Quantitative data suggesting that ice-rafting is an important sedimentary agent in high latitudes has been presented by Kranck (1964). Random occurrences of pebbles in the Prince Gustaf Adolf Sea area are therefore not considered to be indicative of hydraulic conditions.

A sample of possible bedrock outcrop was cored from a water depth of 363 metres on Station 8, at a depth of 48 cm below the bottom. The sample consisted of 8 cm of light grey shale and mudstone. Its firmness and near-horizontal fissility suggest that it was taken from bedrock rather than from a boulder or other detrital fragment. Overlying, grey sandy mud and clay beds may be disaggregated portions of this rock. The sample is similar lithologically to rocks of the Deer Bay Formation, which crop out on nearby Ellef Ringnes Island (Fig. 3).

Composition of Sediment

Sand

Sand grains from the Prince Gustaf Adolf Sea area are composed of quartz, feldspar, rock fragments, foraminiferal tests, and accessory and trace minerals, with quartz being by far the dominant component. Feldspar makes up less than 5 per cent of all but a few samples. Rock fragments consist mainly of limestone and mudstone grains and rarely occur in concentrations of more than 3 per cent. Accessory minerals vary in their concentrations, being generally less than 1 per cent of the total sediment by weight. Foraminiferal tests are considered later in this report (under the heading 'Fauna'). The sand fraction in general is therefore quartz-rich and in most samples is orthoquartzitic.

Quartz grains from the samples are angular to well rounded and have surface textures that are generally either smooth or etched. Grains taken from submarine samples are similar in their morphologies to grains from stream and outcrop samples on Ellef Ringnes, King Christian, and Lougheed Islands. Quartz from some bottom samples (e.g. Samples 12A, 39A, 48A, and 53A, Appendix C) are coated to various extents by oxidized iron minerals. These grains always occur in the yellow-brown layer and probably reflect the same oxidizing conditions as does the mud-size sediment in this layer. Many quartz grains from sub-bottom samples are partly coated with fragments of pyrite cement. Such cement is common in the mudstone formations of Ellef Ringnes, King Christian, and Lougheed Islands and it is inferred that grains with pyrite cement, which occur in submarine samples, were derived from these and similar formations.

There is no apparent orderly variation in the relative abundances of feldspar types over the entire area of study, as determined from a selection of 50 samples, and these abundances are not considered significant to this study. Sodic feldspar is subordinate to potash feldspar in all samples examined but two from Core 58, in Berkeley Trough. Sodic feldspar is the predominant type in this core and may reflect the influence of the Palaeozoic rocks that outcrop on the islands immediately south of that station. Feldspar grains are fragments of typical sanidine, microcline, and sodic plagioclase. They are subangular to subround and no secondary enlargement of grains was noted.

Limestone fragments occur in minor amounts over much of the study area; they reach concentrations greater than 1 per cent of the total non-quartz and feldspar fraction in the western half of the area and as great as 65 per cent in Lougheed Island Basin. These fragments are irregular in shape and are subround to round. They are composed of clastic calcareous grains in clear, sparry cement, which frequently shows good cleavage faces. Core 71, from Lougheed Island Basin, has no limestone fragments in its upper 4 cm, which is clay; at 40 cm, in clay mud, traces of limestone fragments appear; at 55 cm, in muddy sand, limestone fragments amount to 12 per cent of the total non-quartz and feldspar fraction; and at 85 cm, in sandy mud, 29 per cent of that fraction is composed of limestone grains (Appendix C). Core 78, from Lougheed Island Basin, shows a fivefold increase in limestone fragment content from its top to 65 cm, with an accompanying lithologic change from clay mud to clay. The limestone content in Core 80, also in Lougheed Island Basin, decreases by a factor of 3 from the top of the core to 70 cm, where it is composed of cloudy, iron oxide-stained grains in association with abundant chlorite and mica (Appendix C). Core 68, from the north end of Lougheed Island Basin, contains limestone fragments in the amount of 71 per cent of the non-quartz and feldspar fraction at a depth of 15 cm, in clay mud. It is apparent from these data that there has been a continuous supply of limestone detritus to the Lougheed Island Basin area during varying environmental conditions. Limestone is rare in the formations that outcrop on the islands of the area and is found in abundance only in the Palaeozoic rocks of the

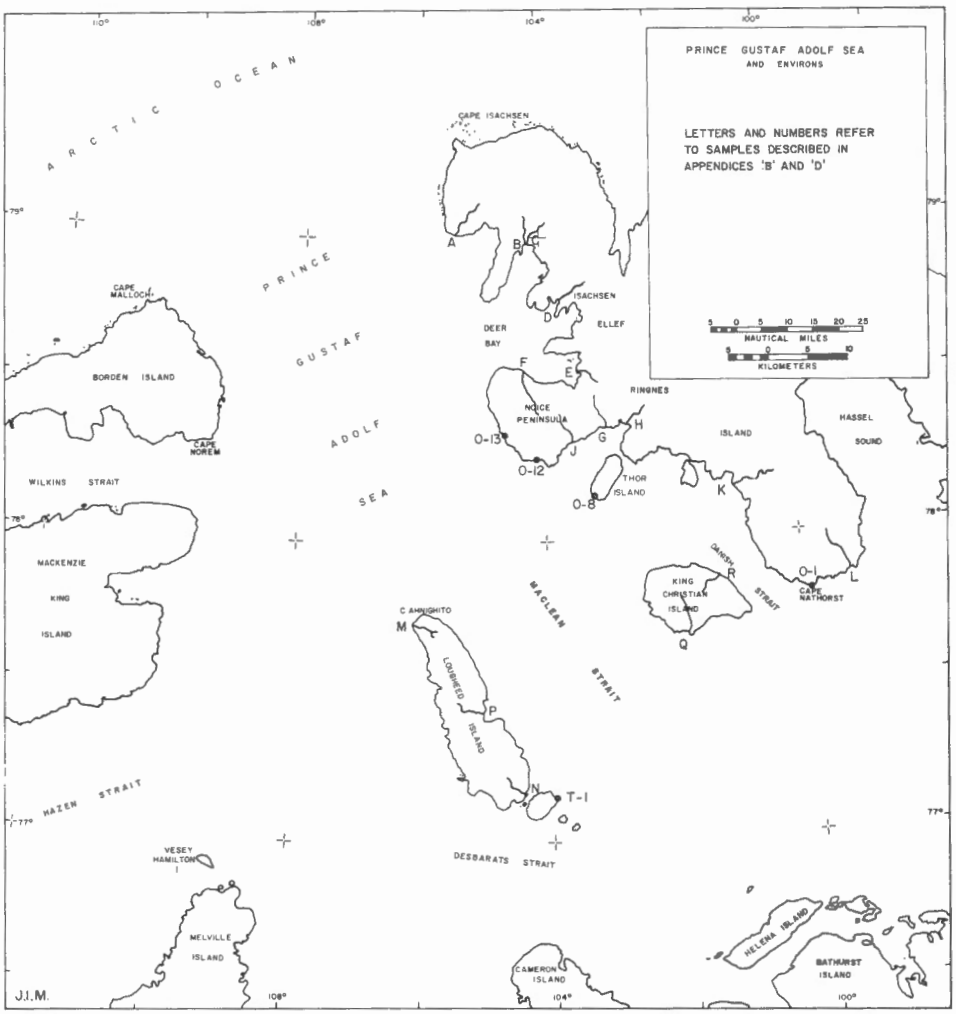

Figure 14. Locations of stream, outcrop, and foreshore samples

Franklin Geosyncline, to the south (Fortier et al., 1963, Map 1103A; Tozer and Thorsteinsson, 1964, Map 1142A; this report, Fig. 3). The presence of limestone detritus can be explained as sediment transported from sources to the south by glacial ice during periods of lower sea level; it is difficult, however, to account for the local abundance of limestone fragments in the tops of cores. Because of unavoidable circumstances, stream samples were not collected from the coasts around Lougheed Island Basin and therefore it is not known whether limestone fragments are being delivered to the sea by streams in the area. Limestone cobbles are common as erratic surface deposits on Lougheed Island and it appears that some of this material must eventually reach offshore areas as sand-size fragments. A more plausible explanation for the offshore sand may be that limestone beds outcrop on the sea floor around Lougheed Island Basin and provide a small but continuous supply of detritus to surrounding areas.

Mudstone fragments were found in sand samples throughout the area of study (Appendix C). These grains are tabular and rounded, but frequently show fissile parting at broken edges. They are composed predominantly of clay-size sediment and have a waxy appearance under 60X magnification. Many mudstone grains contain finely disseminated pyrite and have a colour and lustre similar to those of pyrite; most of the grains, however, are brown to grey. Sand samples taken from streams draining parts of Ellef Ringnes, King Christian, and Lougheed Islands contain similar fragments, and it is considered that the mudstone fragments found in submarine samples originated in the mudstone and shale formations of the area.

Trace amounts of sandstone and igneous rock fragments were observed in a few samples (Appendix C). Exotic rocks, however, comprise a negligible proportion of the sand in samples taken for this study.

Sand samples were separated into heavy and light mineral fractions by the bromoform method. Heavy fractions of each sample were studied to determine any variations in composition. Sediment in the area of study was found to be characterized by a mature suite of heavy minerals, which reflects the composition of heavy mineral suites in outcropping formations of the local islands. Opaque minerals are the most abundant species.

The heavy minerals found most commonly in this study are: ilmenite, magnetite, garnet, zircon, tourmaline, rutile, kyanite, staurolite, pyrite, and oxidized opaque minerals. Oxidized opaque minerals include fragments of pyrite cement, pyrite concretions and aggregates, and magnetite grains, all of which are coated or nearly coated with iron oxide minerals or other minerals, which give the grains a "rusty" appearance. Only trace amounts of leucoxene were noted. Oxidized opaque minerals are the most abundant group and compose an average of 46.9 per cent of the heavy mineral fraction of bottom samples in the area. Ilmenite and magnetite together comprise 19.6 per cent of the heavy minerals. Garnet is found in all samples and has an average abundance for the area of 6.8 per cent of the

total heavy fraction. Tourmaline and rutile are also ubiquitous and have average abundances of 3.5 per cent and 1.4 per cent, respectively. Unoxidized pyrite has an areal average abundance of 3.2 per cent; this mineral is locally very abundant, however, and at Stations 19, 20, 23, and 27 pyrite averages 73.4 per cent of the heavy fraction. Zircon occurs in at least trace amounts in all bottom samples and has an average abundance for the area of 1.8 per cent. Staurolite and kyanite are of local importance only and have average abundances at 18 stations in the Grinnell Ridge area of 1.7 per cent and 1.4 per cent, respectively. A large variety of minor minerals occur in varying but small amounts throughout the area of study. These include augite, diopside, monazite, apatite, sphene, sillimanite, chlorite, hornblende (mostly "common", but some "basaltic"), hypersthene, epidote, olivine, glauconite, enstatite, tremolite, actinolite, gold, gypsum, zoisite, siderite, and andalusite.

The common heavy minerals constitute a suite that is similar to heavy mineral suites from outcrops and stream beds on Ellef Ringnes, King Christian, and Lougheed Islands. Outcrop samples from various formations of different age have similar heavy mineral assemblages (Fig. 15). All of these samples contain a predominant, mature suite of minerals derived from metamorphic and acid igneous rocks and a minor suite of less stable minerals.

Opaque minerals are least abundant over Grinnell Ridge and in this area garnet, zircon, kyanite, and staurolite have their maximum abundances. Sub-bottom samples in the area show similar relative abundances. The area of greatest concentration of these minerals (Fig. 16) coincides with the contour pattern showing increasing median diameter over Grinnell Ridge (Fig. 8). This association suggests that the abundances of garnet, zircon, kyanite, and staurolite are related to median grain size of the sand in which they occur, and that abundance increases with grain size. In Figure 16, maximum abundances of these minerals occur in the area of maximum grain size at the crest of the ridge, and it appears that in that area such a relationship does exist. Elsewhere on Grinnell Ridge, however, abundance of non-opaque minerals is not directly related to median grain diameter. Garnet in samples from Stations 43 and 48, for instance, is two to four times as abundant as garnet in samples from Stations 49 and 57 (Appendix D), although the median grain diameters of the latter two samples are 4 to 5 Phi intervals larger than the median diameters of samples from Stations 43 and 48. Furthermore, sediment with size ranges similar to that on part of Grinnell Ridge occurs elsewhere in the study area and at those stations (e.g., 28, 40, and 64) relative abundances of non-opaque heavy minerals are much less than those on Grinnell Ridge.

The most probable explanation for the high abundances of garnet, kyanite, staurolite, and zircon in the Grinnell Ridge area is that the mineral assemblage reflects the mineralogy of its source rocks, and that the sediment of the area is derived from rock units mineralogically distinct from

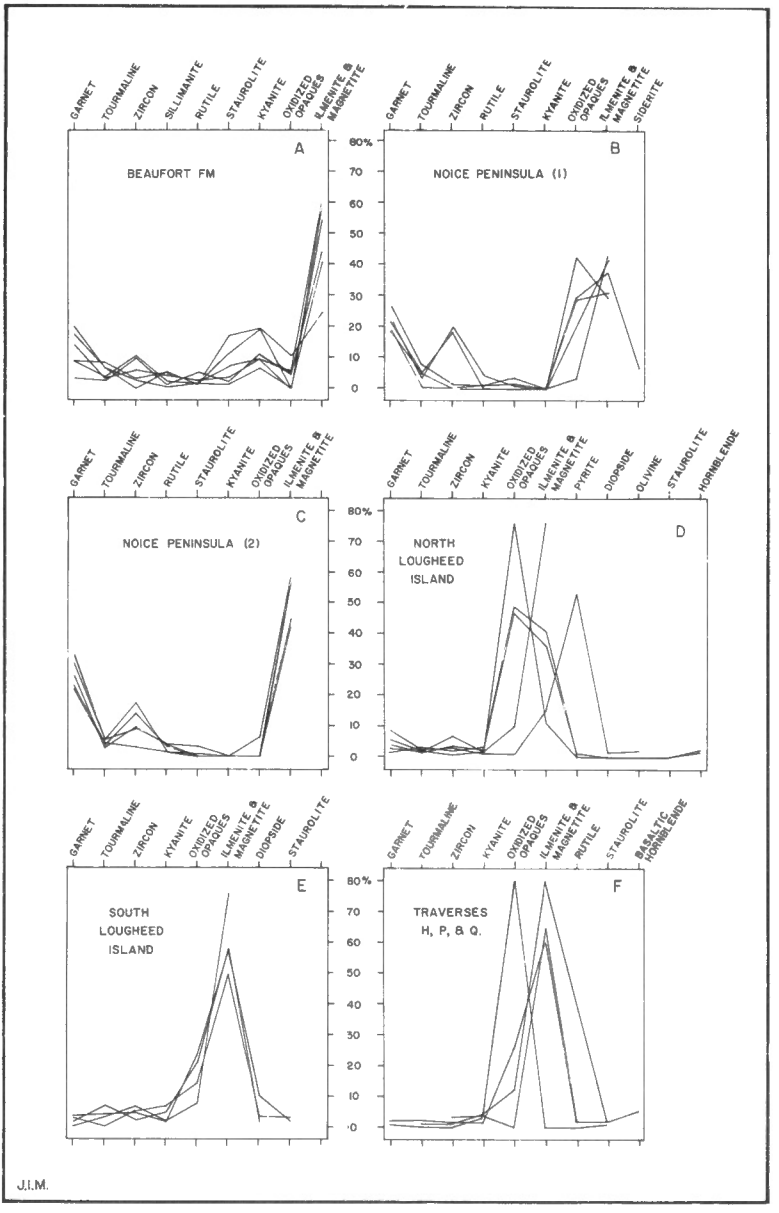

Figure 15. Heavy mineral compositions of stream and outcrop samples. See Figure 14 for location of samples.

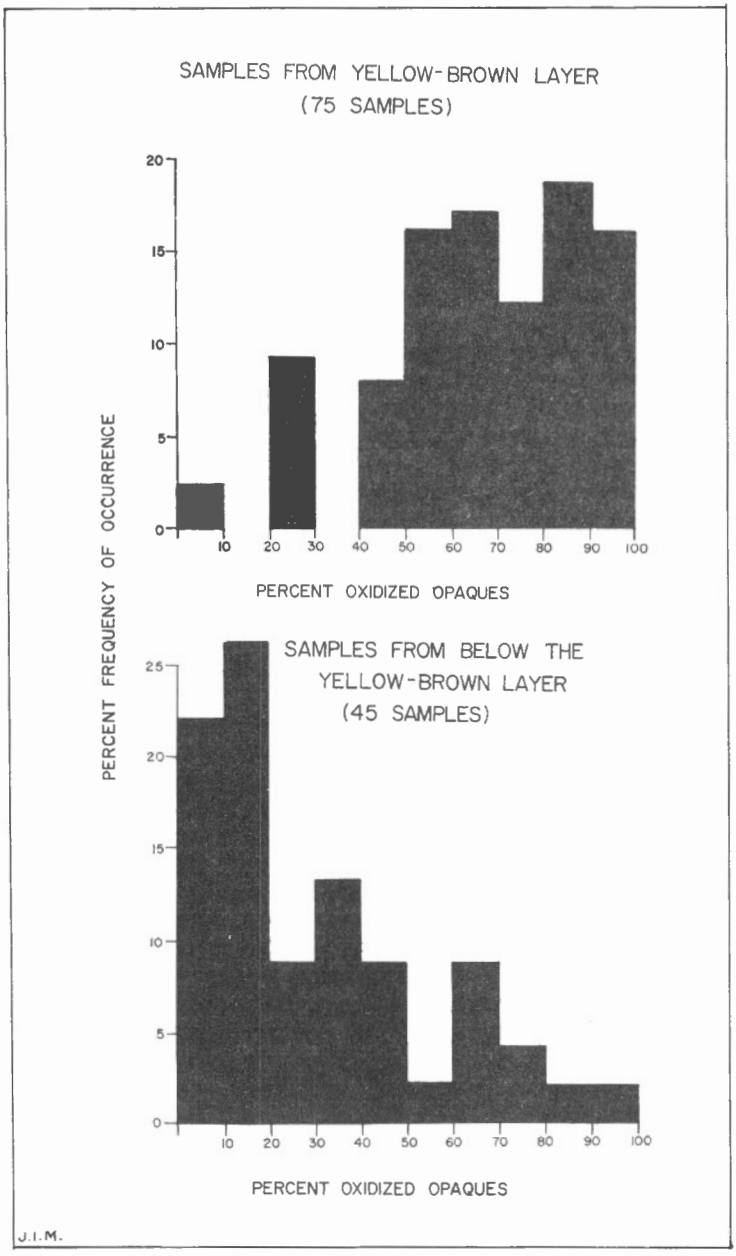

Figure 16. Heavy mineral associations in marine samples

bottom sediment in adjacent areas. Garnet abundances comparable with those of Grinnell Ridge are found elsewhere in the study area only in streams that drain the Isachsen Formation on Noice Peninsula (Fig. 15 B and C). Zircon and staurolite also occur in comparable abundances in these stream beds. Sand derived from the Isachsen Formation on Noice Peninsula contains no kyanite; however, sand derived from formations adjacent to the Isachsen Formation contains 2-3 per cent kyanite. On the basis of mineralogy, it therefore appears that Grinnell Ridge may be underlain in part by beds of the Isachsen Formation.

Although abundance values for kyanite in the sand of the Beaufort Formation (Fig. 3) range between 6 per cent and 19 per cent (Fig. 15 A), only trace amounts of kyanite occur in samples taken from stations off the north coasts of Ellef Ringnes and Borden Islands, where this formation outcrops. Apparently sand-size kyanite is not now transported from land to points as close as 4 km (2.2 miles) offshore. At a depth below the bottom of 9 cm, however, Core 4 contains 7 per cent kyanite. This suggests that Station 4 was located considerably closer to shore at the time of deposition of this sample than it is now. Kyanite abundances in Core 28, off Cape Ahnighito, suggest a similar relation. Kyanite in stream beds on Cape Ahnighito amounts to 3 per cent of the heavy mineral fraction, whereas no kyanite occurs at the top of Core 28, taken from 206 metres of water 6.5 km (3.5 miles) offshore. At a depth of 12 cm, however, this core contains 1.6 per cent kyanite (Appendix D).

Samples from Lougheed Island Basin, Berkeley Trough, the flanks of Grinnell Ridge, and parts of northern Prince Gustaf Adolf Sea contain small proportions of relatively unstable minerals. Stations 5, 6, 7, 8, 9, and 60, between Borden Island and Deer Bay, contain from 1 per cent to 5 per cent hornblende (Appendix D). The hornblende in these samples is not the red-brown "basaltic" variety, but is "common" green hornblende. As Stations 5, 6, 7, 8, 9, and 60 are located in an area that is 111 km (60 miles) north of other significant hornblende occurrences, it is possible that they are receiving sediment from a local source of hornblende-bearing sand. None of the cores at these stations contain significant amounts of hornblende below the present bottom. Cores 74, 76, 77, and 80, in Lougheed Island Basin, contain from 1 per cent to 4 per cent hornblende. Cores from the flanks of Grinnell Ridge (Cores 37, 38, 47, 48, 53, and 55) contain from 2 per cent to 5 per cent hornblende. Hornblende below the bottom at all these stations is rare to non-existent. The areal and topographic unity of cores containing hornblende in the above two areas again suggests that the stations have a common source of sediment supply. "Common" hornblende was observed in concentrations of 1 per cent to 2 per cent in stream and outcrop samples from northern Lougheed Island (Fig. 15 D), where much of the outcropping rock consists of probable Christopher Formation. No other shore samples examined contained more than trace amounts of hornblende. It is therefore possible that beds equivalent to those that outcrop on northern Lougheed Island are the source of the hornblende in Lougheed Island Basin and on the flanks of Grinnell Ridge.

Core 58, from Berkeley Trough at a depth of 382 metres, contains 3.7 per cent blue-green hornblende, a type that was not found elsewhere in the study area. It also contains 3 per cent diopside and traces of "common" hornblende. Nearly all the heavy mineral grains from the top of this core are angular and have a fresh appearance. Hornblende grains have "hack-sawed" ends and only apatite and tourmaline are rounded. In view of its nearness to the Palaeozoic rocks of the Sverdrup Basin, its blue-green hornblende content, and its ragged grain surfaces, together with its sodic feldspar content, some of the sediment in Core 58 was probably derived from land to the south. Abrasion by glacial ice may be in part responsible for the texture of the mineral grains.

Augite occurs in samples from several scattered cores west and north of Lougheed Island, ranging from 1 per cent to 2 per cent in abundance. Core 9, from 2.8 km (1.5 miles) off Ellef Ringnes Island, contains the greatest abundance of augite (Appendix D); this augite may be derived from diabase bodies that outcrop near Isachsen (Fig. 3). No augite was observed in stream and outcrop samples except those near the diabase bodies. Unfortunately, no data on the composition of rocks in the western islands are available, and it is not possible on the basis of present information to infer a source for the augite in central Prince Gustaf Adolf Sea.

Diopside occurs in concentrations of 1 per cent to 11 per cent (Core 71) at several scattered stations in the same general area where augite occurs. The Christopher(?) Formation on northern Lougheed Island contains 1 per cent to 2 per cent diopside (Fig. 15 D) and is the only known possible source for the augite of the marine samples.

Pyrite is the most abundant mineral in bottom sediment from Stations 19, 20, 23, and 27, and is present in concentrations of 6 per cent and 15 per cent at Stations 56 and 57, respectively. Pyrite at all these stations is unoxidized, but is tarnished to varying degrees. All pyrite fragments observed appear to be detrital. Many grains are fragments of interstitial cement and show only slight abrasion on sharp edges. Botryoidal, former cavity fillings and reniform aggregates are common. At Station 57, nearly all the pyrite grains counted were euhedral pyritohedra. At Station 27, the pyrite grains are clean, bright aggregates, whereas at Stations 19, 20, and 23 the grains are slightly tarnished. The latter four stations are located in the area between Lougheed Island and Noice Peninsula (Fig. 16). The areal unity of samples from these stations, together with the fresh, unoxidized aspect of the pyrite contained in them, suggests that the pyrite is being supplied by a local source.

Fresh pyrite was observed in only one outcrop sample, taken from Christopher Formation(?) beds on northern Lougheed Island (Fig. 15 D). Aggregates and euhedra in this sample were bright and fresh and composed 52 per cent of the heavy mineral fraction (Appendix D). Samples taken from a stream bed 1.5 km (1 mile) downstream from this outcrop contained only

oxidized pyrite. Such outcrops may occur on the sea bottom in the pyrite-rich area off Noice Peninsula described in Figure 16; if this is the case, it is apparent that oxidation has had little effect on the pyrite after its deposition in the yellow-brown beds.

While samples from the tops of cores, in the yellow-brown layer, are deficient in fresh pyrite, samples from the underlying, dark-coloured beds are comparatively rich in pyrite. In central Prince Gustaf Adolf Sea, cores taken at Stations 5, 7, 22, 60, and 67 contain as much as 98 per cent pyrite aggregates (Appendix D) in sub-bottom layers. Cores from Stations 70, 71, and 72, between Cape Ahnighito and Mackenzie King Island, contain as much as 44 per cent pyrite in sub-bottom layers; Core 72, however, from 22 km (12 miles) off Mackenzie King Island, also contains 36 per cent oxidized opaque minerals in a muddy sand layer 40 cm below the bottom. In Lougheed Island Basin, sand in Core 77 is 73 per cent polyspherical aggregates of pyrite at a sub-bottom depth of 26 cm; at 110 cm, in a sandy mud layer, there is 23 per cent pyrite and 53 per cent oxidized opaque minerals, most of which appear to be after pyrite. Core 78, which at its top contains no fresh pyrite, but instead contains 17 per cent oxidized pyrite, has at 28 cm 72 per cent pyrite and no oxidized opaques. Similarly, Core 79, from the west end of Cameron Island Ridge, contains 99 per cent oxidized pyrite aggregates at its top, but 37 per cent fresh pyrite and no oxidized opaques at 51 cm. On the flanks of Grinnell Ridge, an area in which pyrite occurs in bottom sediments, Cores 42 and 48 contain sub-bottom concentrations of pyrite of 63 per cent and 76 per cent, respectively. Core 41, off the south end of Lougheed Island in Desbarats Strait, contains 40 per cent oxidized opaques and no pyrite at the top, whereas at a sub-bottom depth of 13 cm it contains 70 per cent bright pyrite aggregates.

There is a general decrease in abundance of oxidized opaque minerals with depth below the bottom (Fig. 17). While this relationship does not hold true in all cases, notably in those samples from the pyrite-rich areas previously described, the yellow-brown layer contains much higher abundances of oxidized opaque minerals than do the underlying beds. Conversely, there is a general decrease in oxidized pyrite content with depth below the bottom. This decrease in oxidized opaque mineral abundance coincides generally with the transition from yellow-brown bottom sediment to darker coloured sediment at depth. Figure 17 shows that oxidized opaque mineral grains are more abundant in the yellow-brown layer than in lower beds, and furnishes supporting evidence for the hypothesis stated earlier in this report that the colour of the yellow-brown layer is a result of oxidation of iron minerals. It further supports the idea that oxidation, and hence probably oxygenation, has affected the upper, yellow-brown, layer, more than the beds below.

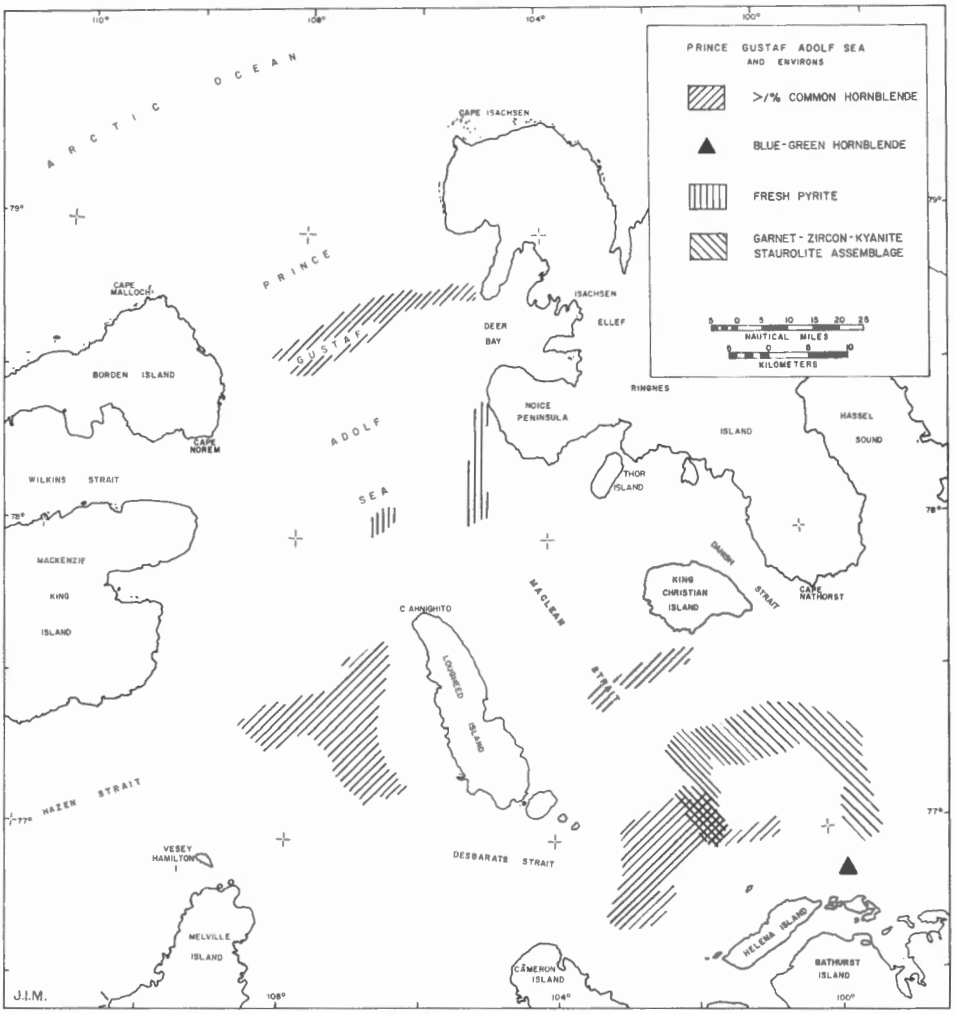

Figure 17. Vertical distribution of oxidized opaque minerals in core samples. Oxidized opaque values are shown as percentages of total opaque mineral abundances

Mud

Mud samples were examined optically and by X-ray diffractometer to determine their mineralogical composition. Quartz was found to be the dominant mineral type in all samples and was present in all size classes. Very small proportions (less than 1 per cent) of staurolite, garnet, tourmaline, and other heavy minerals common in the sand fraction were identifiable in size grades as small as fine silt (7ϕ). X-ray analyses made on 40 samples from throughout the area of study indicated that size grades below 6ϕ are composed predominantly of quartz, kaolinite, and illite. Montmorillonite was present in 11 scattered samples. Quantitative estimates made on the basis of the areas included under the 7, 10, and 15 Angstrom peaks resulted in the following relative abundances of the major clay mineral types: kaolinite 68 per cent, illite 26 per cent, and montmorillonite (average contents of 10 samples, excluding Station 36) 7 per cent. There was no apparent relationship between montmorillonite abundance and distance from shore or topography. Clay minerals taken from samples at various levels below the bottom show no change in relative abundances of the species. Clay mineral analyses on five samples of mudstone outcrop from Ellef Ringnes and Lougheed Islands showed kaolinite/illite ratios of approximately 2.0. Compositions of submarine mud samples from Prince Gustaf Adolf Sea, therefore, are similar to compositions of outcrops on nearby islands.

The bottom sample from Station 36, in Danish Strait (Fig. 4), contained 67 per cent kaolinite and 21 per cent "montmorillonite", with only 2 per cent illite. The "montmorillonite" in this sample expanded to 17 Angstroms upon glycolation and appears to be similar to montmorillonite-like mixtures of chlorite and degraded illite, described by Griffin and Goldberg (1963, p. 735), which have resorbed potassium in the marine environment. Core 36, from a depth of 225 metres, consisted of 18 centimetres of medium grey clay mud, which was logged in the field as "mottled dark grey and yellow-brown mud". Three months after collection this core was mottled over its outer surface with bright orange-yellow, very finely divided, limonitic minerals. On examination, the interior of the core was observed to contain irregular mottlings of very fine, black, subspherical aggregates, which later oxidized to rusty yellow. These colour changes were due to the oxidation of finely divided iron minerals, which probably occurred originally as sulphide compounds. Such minerals are stable in reducing conditions and when present in marine sediments generally indicate a lack of ventilation of the overlying water. Ericson, et al. (1961, pp. 204-205) pointed out, however, that many iron sulphide compounds in marine sediments are probably formed in reducing environments produced by the metabolic activity of heterotrophic bacteria.

Gravel

Gravelly beds and isolated pebbles occur in a number of cores. A small proportion of this gravel is composed of fragments of igneous and

metamorphic rocks of distant origin; the greater part, however, consists of pebbles of lithologies similar to those of rocks that outcrop in or near the Prince Gustaf Adolf Sea area. The most common lithologies, in their order of abundances, are: greenish grey, fine, quartzose sandstone; grey shale and mudstone; and dark brown mudstone. Limestone pebbles were observed in one core (Core 79). There can be little doubt that large fragments of well-lithified rocks lie on the bottom of Prince Gustaf Adolf Sea, as ice-rafted boulders have been observed on the surface in the area. Also, occasional severe damage to core bits attests the presence of very hard materials on the bottom.

Cores 5, 6, 17, 18, 20, 23, and 29, in the Lougheed Island Ridge-Danish Strait Valley area, contain pebbles of grey to black shale and greenish grey, micaceous sandstone. Many of the shale pebbles are soft and friable, but have been only slightly rounded by abrasion. Cores 62, 68, 70, and 71, in the western half of the study area north of Lougheed Island Basin, also contain beds with dark coloured shale and greenish grey, quartzose sandstone pebbles. All of these fragments are slightly rounded. Core 78, on the shore-face southwest of Lougheed Island, contains pebbles of dark grey clay shale in poorly sorted beds of gravelly clay. Fine pebbles of grey sandstone occur near the base of Core 77, in Lougheed Island Basin.

Core 79, at the western end of Cameron Island Ridge, contains fine pebbles of shale, limestone, and metamorphic rocks in a pebbly, sandy mud layer 88 cm thick. This is the only known occurrence of limestone pebbles in submarine samples from the area.

Cores 32 and 38, on the flanks of Grinnell Ridge, contained fine, rounded pebbles of greenish grey sandstone in beds of sandy mud. Core 53, at the east end of Desbarats Trough, contained pebbles of the same lithology.

Lithologies found in pebbles of the bottom sediments in the study area are similar to lithologies of rocks that occur on the adjacent islands. Shale and mudstone formations underlie much of Ellef Ringnes, King Christian, Lougheed, and Mackenzie King Islands and probably parts of the surrounding sea floor. Grain morphologies indicate that the shale and mudstone pebbles have undergone little abrasion and hence have not been transported over the bottom for great distances. Much of this material is probably, therefore, of local derivation.

Tozer and Thorsteinsson (1964, pp. 136-146) described beds from the Mould Bay Formation, which outcrops as far east as Mackenzie King Island, that contain greenish grey sandstone lithologies similar to that of the pebbles found in submarine samples of the Prince Gustaf Adolf Sea area. Greenish grey, quartzose sandstone was also observed on southern Cameron Island and on the coasts of some of the Berkeley Islands. Specimens collected from these areas during refuelling stops are remarkably similar to pebbles that occur in bottom sediments 200 km (108 miles) to the northwest. If some

of the pebbles were derived from rocks of the Franklin Geosyncline (Fig. 3), as lithologies in the Berkeley Islands suggest, a northward, and oceanward, direction of transport is implied. Such movement could have taken place in glacial ice during times of lower sea level. It is more likely, however, that the sandstone pebbles are of local origin and have been derived from outcrops now on the sea bottom or on the adjacent islands.

An alternative source for the sandstone is in the distant land areas where much of the polar ice that enters Prince Gustaf Adolf Sea originates. The homogeneity of composition of the pebbles indicates that this is not, however, the case.

The mixed lithologic association of Core 79 probably is a partly reworked, shallow-water deposit of glacial origin. The limestone pebbles may be of local derivation, as may be sand-size limestone grains concentrated in the Lougheed Island Basin area; the igneous and metamorphic rock fragments, however, originated in distant sources and probably were brought into the area by glacial transportation.

FAUNA

Microfaunas collected from marine sediments in the western Queen Elizabeth Islands have been studied and reported on by Wagner (1962, 1964), Vilks (1964), and Marlowe and Vilks (1963). Preliminary data on the foraminifera of Prince Gustaf Adolf Sea (G. Vilks, Bedford Institute of Oceanography, personal communication) indicate a gradual decrease in planktonic, calcareous forms southward from the Arctic Ocean to about the latitude of Lougheed Island. There is an increase in arenaceous forms over the same distance. The planktonic population is characterized by Globigerina pachyderma, a species that does not occur in recent sediments of the area above a depth of 200 metres. At this depth at the north end of Prince Gustaf Adolf Sea, Collin (1961) reported a relatively warm water layer of probable Atlantic origin. Vilks (personal communication, 1965) reported that cores from Desbarats Strait (Stations 41, 46, and 52) contain arenaceous forms at their tops but calcareous species at depth. As the modern calcareous fauna shows a preference for depths of 200 metres or greater, Vilks inferred that depths in Desbarats Strait have been greater in the past than they are at present. Alternatively, the preferred layer of water that appears to exist at about 200 metres elsewhere in the area of study may have flowed over the low sill west of Desbarats Strait at some time in the past. A microfaunal list provided by Vilks is appended to this report (Appendix E).

Vilks reports no foraminifera from samples taken from below the yellow-brown layer. Core 62, from a depth of 151 metres off Cape Norem, contains the only faunal remains found below the yellow-brown layer. In the interval from 24 to 29 cm below the bottom (1 to 5 cm below the yellow-brown layer), in a grey, sandy mud bed, abundant calcareous worm burrows and small (4-5 mm) pelecypod valves were observed.

SUMMARY AND CONCLUSIONS

Geological data from the Prince Gustaf Adolf Sea area support the hypothesis of Fortier and Morley (1956) that islands of the Canadian Arctic Archipelago are parts of a submerged, continental terrain. Submarine landforms indicate the former existence of a subaerial drainage pattern, which had its origins south of the study area and emptied into the Arctic Ocean. Present islands represent former drainage divides and highlands; some similar features are not now emergent, but exist as ridges and banks under the sea. Gently sloping headlands, such as Cameron Island Ridge and Lougheed Island Ridge, and a well defined island slope suggest that the sea and shoreline approached dynamic equilibrium at a level 300 to 400 metres below present sea level. The former existence of glacial ice in the area is inferred from the presence of trough-like, flat-bottomed, submarine valleys. Sedimentary structures indicate that marked changes in the sedimentary environment have occurred in the Prince Gustaf Adolf Sea area.

Quiescent, probably slightly reducing conditions prevailed during a period represented by lower, grey-coloured beds. During this time water depths were shallower than at present and bottom currents were more effective. This sediment appears to have been derived from within the area and there is little indication of transportation of detritus from exotic sources. Bottom sediments were poorly ventilated and in the Lougheed Island Basin area may have been restricted from the open sea. Deposition in most deep areas was quiet. Cyclical bedding in the Lougheed Island Basin area suggests a seasonal, perhaps glacial, control of sedimentation in that area. No microfaunal remains were found in the lower beds.

Following the deposition of the grey beds, yellow-brown sediment accumulated in the Prince Gustaf Adolf Sea area. The deposition of this sediment has continued to the present. The mineralogy of these beds indicates that oxidizing conditions prevailed during the time of their deposition. The absence of bedding and the presence of abundant microfaunal remains suggest that reworking of sediment by burrowing organisms became effective at this time. A microfauna described as being typical of open Arctic Ocean waters (Vilks, p. 46, this report) occurs at depths of 200 metres and lower. This depth agrees with the depth given by Collin (1961) for a warm layer of "Atlantic" water at the north entrance of Prince Gustaf Adolf Sea. It is therefore inferred that the change to oxidizing conditions on the bottom was the result of the incursion of this "Atlantic" water mass, which exerted more and more influence on Prince Gustaf Adolf Sea as sea level rose. Thickness values for the upper, yellow-brown layer are taken in this report as an index of the relative effectiveness of oxidation in the area. These values indicate that oxidation in the western half of the area has been more effective than in the eastern half; therefore, aerated bottom conditions may have existed in the Prince Gustaf Adolf Sea-Byam Martin Channel area longer than they have in the Grinnell Ridge-Penny Strait area. Preliminary faunal data from Vilks

(p. 46, this report) imply that "Atlantic" water from the Arctic Ocean formerly passed through Desbarats Strait, although samples from recent sediment show that no fauna typical of this water mass are now being deposited in that area. This may be an indication that "Atlantic" water moving down the east coast of Lougheed Island flowed preferentially through Desbarats Strait and southward through Byam Martin Channel. At a sea level 100 metres below the present, Grinnell Ridge would obstruct currents moving toward it from the west. It therefore appears that water from Prince Gustaf Adolf Sea may have circulated through Byam Martin Channel before circulation through Penny Strait began.

Recent sediment in the area appears to be derived from streams flowing into the sea from land areas, from submarine outcrops, and from wind-blown detritus from the islands. Floating ice contributes an unknown proportion of the sediment. Bottom currents are effective in sorting the sediment and are most effective in shallow areas. Little mud is deposited on the crest of Grinnell Ridge, for instance, as opposed to muddy areas in the deeper, central Prince Gustaf Adolf Sea. Suspended-load sediment may be carried by debouching streams to offshore areas; however, there is no indication that bedload-size material is at present transported more than a short distance from shore. Compositions of sand and gravel fractions indicate that much of this material is derived from local sources on the sea bottom. Compositional similarities between sea-bottom sands and terrestrial outcrops suggest that some formations that occur ashore also underlie the sea.

REFERENCES

Belov, N.A., and Lapina, N.N.
1958: New data on the stratigraphy of the bottom sediments of the Arctic Basin of the Northern Arctic Ocean; Dokladi, Akedemii Nauk, S.S.S.R., vol. 122, p. 115 (Translated by J.H. Bradley).

Blackadar, R.G.
1963: Dumbells Dome, Ellef Ringnes Island; in Geology of the north-central part of the Arctic Archipelago, Northwest Territories (Operation Franklin); Geol. Surv. Can., Mem. 320, pp. 558-562.

Canadian Hydrographic Service
1958: Cornwallis Island to Lougheed Island; Chart 7095.

1965: Atlantic coast tide and current tables; p. 219.

Collin, A.E.
1961: Oceanographic activities of the Polar Continental Shelf Project; J. Fish. Res. Bd., vol. 18, pp. 253-258.

Craig, B.G., and Fyles, J.G.
1960: Pleistocene geology of Arctic Canada; Geol. Surv. Can., Paper 60-10.

Eaton, R.M.
1962: Borden Island Decca chain hydrographic sounding chart, southern sheet; Can. Hydrog. Serv., Dept. Mines Tech. Surv., Ottawa, File No. 32-66-LSC.

Ericson, D.B., et al.
1961: Atlantic deep-sea sediment cores; Bull. Geol. Soc. Am., vol. 72, pp. 193-286.

Fortier, Y.O., et al.
1963: Geology of the north-central part of the Arctic Archipelago, Northwest Territories (Operation Franklin); Geol. Surv. Can., Mem. 320.

Fortier, Y.O., and Morley, L.W.
1956: Geological unity of the Arctic Islands; Trans. Roy. Soc. Can., Ser. 3, vol. 1, Canadian Committee on Oceanography, pp. 3-12.

Glenister, B.F., and Thorsteinsson, R.
1963: Southern Lougheed Island; in Geology of the north-central part of the Arctic Archipelago, Northwest Territories (Operation Franklin); Geol. Surv. Can., Mem. 320, pp. 571-575.

Greiner, H.R.
1963: Malloch Dome and vicinity, Ellef Ringnes Island; in Geology of the north-central part of the Arctic Archipelago, Northwest Territories; Geol. Surv. Can., Mem. 320, pp. 563-571.

Griffin, J.J., and Goldberg, E.D.
1963: Clay-mineral distribution in the Pacific Ocean; in The Sea, vol. 3: New York, Interscience Publishers, pp. 728-741.

Hayes, J.R., and Klugman, M.A.
1959: Feldspar staining methods; J. Sed. Petrol., vol. 29, pp. 227-232.

Heywood, W.W.
1957: Isachsen area, Ellef Ringnes Island, District of Franklin, Northwest Territories; Geol. Surv. Can., Paper 56-8.

1959: Ellef Ringnes, Amund Ringnes, Cornwall and Lougheed Islands, Northwest Territories; Geol. Surv. Can., Map 14-1959.

Hjulstrom, F.
1938: Transportation of detritus by moving water; in Recent marine sediments; Soc. Econ. Paleontologists and Mineralogists, Spec. Publ. No. 4, pp. 5-31.

Horn, D.R.
1963: Marine geology, Peary Channel, District of Franklin: Polar Continental Shelf Project; Geol. Surv. Can., Paper 63-11.

Kranck, K.
1964: Sediments of Exeter Bay, District of Franklin; Bedford Inst. Oceanography, Report 64-15.

Krumbein, W.C., and Pettijohn, F.J.
1938: Manual of sedimentary petrography; New York, Appleton-Century-Crofts, Inc., 549 pp.

Leslie, R.J.
1963: Sedimentology of Hudson Bay, District of Keewatin; Bedford Inst. Ocenography, Report 63-4.

McLaren, D.J.
1963: Meteorologist Peninsula Dome, Ellef Ringnes Island; in Geology of the north-central part of the Arctic Archipelago, Northwest Territories (Operation Franklin); Geol. Surv. Can., Mem. 320, pp. 552-558.

Marlowe, J.I.
1964: Marine geology, western part of Prince Gustaf Adolf Sea, District of Franklin: Polar Continental Shelf Project; Bedford Inst. Oceanography, Report 64-9.

Marlowe, J.I., and Vilks, G.
1963: Marine geology, eastern part of Prince Gustaf Adolf Sea, District of Franklin: Polar Continental Shelf Project; Geol. Surv. Can., Paper 63-22.

Pelletier, B.R.
1962: Submarine geology program, Polar Continental Shelf Project, Isachsen, District of Franklin; Geol. Surv. Can., Paper 61-21.

1964: Development of submarine physiography in the Canadian Arctic and its relation to crustal movements; Bedford Inst. Oceanography, Report 64-16.

Pettijohn, F.J.
1957: Sedimentary rocks, 2nd ed.: New York, Harper and Bros., 718 pp.

Price, W.A.
1954: Shorelines and coasts of the Gulf of Mexico; in Gulf of Mexico, Its Origin, Waters, and Marine Life; U.S. Fish and Wildlife Serv., Fishery Bull. 89, vol. 55, pp. 39-65.

1955: Correlation of shoreline type with offshore bottom conditions; Dept. Oceanog., Agr. and Mechan. College of Texas, Mimeo. Report, Ref. 55-8T.

Roots, E.F.
1963: Physiography of Cornwall, Lougheed, Amund Ringnes, and Ellef Ringnes Islands; in Geology of the north-central part of the Arctic Archipelago, Northwest Territories (Operation Franklin); Geol. Surv. Can., Mem. 320, pp. 522-528.

Shepard, F.P.
1963: Submarine geology, 2nd Ed.; New York, Harper and Row, 557 pp.

Stefansson, V.
1916: Tidal, geographical, and geological observations on and around Ellef Ringnes, Lougheed, and King Christian Islands; unpub. personal journal, Geol. Surv. Can.

1921: The friendly Arctic; New York, MacMillan, 784 pp.

Sverdrup, O.N.
1904: New land; four years in the Arctic regions; London, Longmans, Green and Co., 2 vols.

Taylor, A.
1955: Geographical discovery and exploration in the Queen Elizabeth Islands; Geogr. Branch, Dept. Mines Tech. Surv., Mem. 3, 172 pp.

Terry, R.D., and Chilingar, G.V.
1955: Summary of "Concerning some additional aids in studying sedimentary formations", by M.S. Shvetsov; J. Sed. Petrol., vol. 25, pp. 229-234.

Thorsteinsson, R., and Tozer, E.T.
1960: Summary account of structural history of the Canadian Arctic Archipelago since Precambrian time; Geol. Surv. Can., Paper 60-7.

Tozer, E.T.
1960: Summary account of Mesozoic and Tertiary stratigraphy, Canadian Arctic Archipelago; Geol. Surv. Can., Paper 60-5.

Tozer, E.T., and Thorsteinsson, R.
1964: Western Queen Elizabeth Islands, Arctic Archipelago; Geol. Surv. Can., Mem. 332.

Twenhofel, W.H., and Tyler, S.A.
1941: Methods of study of sediments; New York, McGraw-Hill, 183 pp.

Vilks, G.
1964: Foraminiferal study of East Bay, Mackenzie King Island, District of Franklin (Polar Continental Shelf Project); Geol. Surv. Can., Paper 64-53.

Wagner, F.J.E.
1962: Faunal report, submarine geology program, Polar Continental Shelf Project, Isachsen, District of Franklin; Geol. Surv. Can., Paper 61-27.

1964: Faunal report - II, marine geology program, Polar Continental Shelf Project, Isachsen, District of Franklin; Bedford Inst. Oceanography, Report 64-1.

APPENDICES

APPENDIX A

Descriptions of cores, based on examination by binocular microscope

Core No.	Depth of Water (Metres)		Description (Top to Bottom) *
1	399	0-5 cm	Clay mud, yellow-brown; abundant calcareous foraminifera
		5-8	Sandy mud, grey-brown
		8-24	Sandy mud, grey
2	463	0-6 cm	Clay, yellow-brown; frequent calcareous foraminifera; interlaminated with underlying unit from 2-6 cm
		6-19 cm	Clay, medium grey
3	477	0-21 cm	Clay mud, yellow-brown; rare, 2 mm rock fragments; abundant calcareous foraminifera to 17 cm; 4-mm pelecypod valve at 5 cm
		21-63 cm	Clay mud, medium grey
4	199	0-8 cm	Clay, yellow-brown; rare 1/2-4 mm rock fragments
		8-12	Muddy sand, yellow-brown; rare, broken calcareous shell material; rare wood splinters and iron oxide-stained rock fragments
5	394	0-9 cm	Clay, yellow-brown; abundant calcareous foraminifera; interlaminated with underlying unit from 7-9 cm
		9-11 cm	Clay, dark grey, base sharp
		11-21 cm	Clay, light brown; grades sharply into grey-brown in middle of unit; base sharp
		21-29	Sandy mud, light grey; base sharp
		29-57	Clay mud, dark grey; frequent rock granules; siltstone pebble, 1.5 cm diameter, 10 cm from base; very finely laminated

* For definitions of lithologic terms, see Figure 13.

Core No.	Depth of Water (Metres)		Description (Top to Bottom)
6	392	0-15 cm	Clay, yellow-brown, frequent calcareous foraminifera; 2 mm-thick, grey clay layer at 6 cm; base transitional
		15-42	Clay mud, dark grey; 1.5 cm pebbles of dark brown, waxy siltstone irregularly scattered throughout; 1.5 cm pebbles of light greenish grey clay at 32 cm
7	488	0-10 cm	Clay, yellow-brown; 3 per cent silt and very fine sand (rock fragments) at 0-4 cm; abundant calcareous foraminifera; light tan, round, 1/4 mm-diameter mottlings, probably filled burrows, at 0-4 cm; base sharp
		10-37 cm	Clay mud, medium grey
8	363	0-15	Clay mud, yellow-brown; slightly mottled
		15-46	Clay, dark grey; very finely laminated
		46-48	Sandy mud, dark grey
		48-56	Mudstone, light grey; fissile, firm; possible bedrock
9	264	0-18 cm	Clay mud, yellow-brown; grades to grey at 12-18 cm
		18-70 cm	Clay, medium grey; thin flat bedding; becomes slightly sandy at 50-70 cm
10	214	0-20 cm	Clay, light brown; faint, dark brown, subhorizontal, colour banding; interlaminated with dark grey mud at 17-20 cm
		20-23	Muddy sand, orange-brown; very fine; limonitic
		23-54	Clay, dark grey
11	310	0-23	Clay mud, yellow-brown; 5 mm-thick layers of iron oxide-stained mud at 18 cm and 20 cm
		23-89	Clay mud, dark grey to black
		89-94	Muddy sand, white, quartzose, medium
12	374	0-12	Clay, yellow-brown; abundant calcareous foraminifera
		12-28	Clay, medium grey; faint, 1 mm-bedding
		28-41	Clay mud, medium grey; fine pebbles scattered throughout; faint, 1 mm-thick bedding

Core No.	Depth of Water (Metres)		Description (Top to Bottom)
13	421	0-4 cm	Clay, yellow-brown; abundant calcareous shell fragments
		4-8	Clay, grey
		8-14	Sandy mud, grey
		14-22	Clay mud, grey; occasional granules unconsolidated, brown mud
14	495	0-14	Clay, yellow-brown
		14-27	Sandy mud, medium grey; 2 cm-thick lens of light grey, muddy sand at 24 cm
15	209	0-8	Mud, yellow-brown; scattered medium-grained sand; thoroughly burrowed; calcareous worm tube 1.5 cm long at 6.5 cm; horizon of 2-3 mm rock fragments at 7 cm
		8-12	Mud, grey; finely laminated
16	354	0-9	Clay, yellow-brown; frequent fine to medium rock fragments; frequent calcareous foraminifera; interlaminated with underlying unit at 5-9 cm
		9-36	Clay, medium grey; laminated; occasional, fine to medium rock fragments
17	383	0-13	Clay mud, yellow-brown; interlaminated with underlying unit at base
		13-27	Clay mud, grey, laminated
		27-61	Muddy sand, grey; slightly gravelly, contains scattered pebbles as large as 3 cm; most abundant pebbles black shale, few grey-green sandstone, one brown sandstone
18	498	0-16	Clay mud, yellow-brown; slight, irregular, dark mottling
		16-21	Clay mud, yellow-brown; dark, subhorizontal, colour banding; laminated
		21-69	Clay mud, medium grey grading to dark grey at base; interlaminated grey layers (1-3 mm thick) and black layers (0.5 mm thick)
		69-70	Clay, light grey
		70-74	Sandy mud, dark grey; 3 cm pebble of greenish grey, micaceous sandstone at base

Core No.	Depth of Water (Metres)		Description (Top to Bottom)
19	391		Mud, yellow-brown; lower part of core lost, remainder treated as snapper sample
20	327	0-10 cm	Clay mud, yellow-brown
		10-30	Sandy mud, slightly gravelly-grey
21	355	0-13	Clay mud, yellow-brown; frequent calcareous foraminifera; base sharp
		13-47	Clay mud, grey; massive
22	440	0-5	Clay, yellow-brown; frequent rock fragments, calcareous foraminifera, shell fragments, at 0-2 cm; interlaminated with grey clay at 1.5 cm, laminae 2-3 mm thick
		5-6	Clay, grey; faint, 1/2-1 mm-thick, yellow-brown laminae
		6-12	Clay mud, grey; becomes sandy to base
		12-17	Muddy sand, grey; fine; massive
23	512	0-9 cm	Clayey sand, yellow-brown
		9-25	Clayey sand, medium grey; massive
		25-29	Muddy sand, medium grey; 1 cm-thick zone of dark grey shale fragments at 25 cm
24	326	0-27	Mud, yellow-brown; fine to medium grain, quartz and rock fragments scattered throughout; rare pebbles black shale
		27-38	Sandy mud, medium grey; massive; abundant, irregularly scattered, pebbles of black and dark grey shale
25	236	0-6	Clay mud, yellow-brown; frequent coarse sand- and granule-size quartz and rock fragments
		6-11	Clay mud, grey; very thin bedded; few scattered granules of grey-green sandstone at base
26	332	0-17 cm	Mud, yellow-brown; colour-banded in 3 mm-thick layers with brown mud at 10-17 cm
		17-27	Mud, light grey; slightly, very fine, sandy at 24-26 cm; 5 mm-thick layer of iron oxide-stained mud at 26.5 cm

Core No.	Depth of Water (Metres)		Description (Top to Bottom)
26 (cont'd)	332	27-42	Sandy mud, medium grey; laminated; 3 cm pebble of grey-green sandstone at base
27	474	0-7	Clay, yellow-brown; frequent corroded, calcareous shell fragments
		7-12	Sandy clay, light grey; occasional rock fragments; laminated
28	206	0-7	Muddy sand, yellow-brown; bedding graded
		7-10	Sand, medium grey; fine; matrix silty mud; poorly sorted except at 9-10 cm; abundant coarse and very coarse quartz grains scattered throughout
29	360	0-8	Sandy mud, yellow-brown; reddish brown at 2-5 cm
		8-18	Sandy mud, medium grey; very thin bedded; fine pebble of grey-green sandstone at 11 cm
30	497	0-8 cm	Sandy mud, yellow-brown; abundant aggregates unconsolidated mud scattered throughout
		8-12	Muddy sand, medium grey; very fine; 1.5 cm, flat pebble of light grey, arkosic sandstone with highly altered feldspar at 8 cm
31	572	0-15	Clay, yellow-brown
		15-30	Clay mud, medium grey; laminated
32	323	0-9	Clay, yellow-brown
		9-14	Sandy mud, grey; occasional granules black shale
33	281	0-5	Clay mud, yellow-brown, interlaminated at base with underlying unit
		5-20	Sandy mud, grey; contains few small grey shale pebbles
34	363	0-12	Clay mud, brown; contains interlaminated, flat lenses of light brown and grey mud
		12-30	Muddy sand, grey; iron oxide-stained at 12-13 cm

Core No.	Depth of Water (Metres)		Description (Top to Bottom)
35	120	0-11 cm	Sandy mud, grey
36	225	0-18	Clay mud, grey; occasional wood fragments; approximately 20 per cent black, loose, subspherical aggregates, probably iron sulphides; outside of core mottled with iron oxides; 5 mm-diameter fragment of algal mat at 9 cm; when core was fresh, was logged as "mottled dark grey and yellow-brown mud"
37	250	0-10	Clay mud, yellow-brown; occasional rock fragments 1-2 mm diameter, rare medium to coarse quartz grains
		10-14	Muddy sand, brown; compact
38	303	0-7	Clay mud, brown
		7-34	Sandy mud, grey; contains greenish grey sandstone pebbles as large as 3 cm
39	315	0-14 cm	Clay mud, brown; interlaminated with underlying unit at 9-14 cm
		14-51	Clay mud, grey; laminated
40	316	0-4	Sandy clay, yellow-brown; sand content increases to base
		4-11	Muddy sand, grey; rare wood grains
		11-21	Clay mud, grey; approximately 15 per cent fine, quartz sand at 11-14 cm; thin-bedded; sandy layers, 1/2-1 cm thick, at 14-19 cm
41	133	0-8	Mud, yellow-brown; sand grains moderately stained with iron oxides
		8-12	Clay, light grey, laminated
		12-24	Clay, grey
42	332	0-15	Clay mud, brown; grades downward to grey-brown; abundant arenaceous foraminifera
		15-20	Clay mud, light red-brown; contains laminae of very fine sand; base sharp
		20-30	Sandy mud, grey; grades downward to clean, quartz sand at base

Core No.	Depth of Water (Metres)		Description (Top to Bottom)
43	218	0-6 cm	Clay mud, yellow-brown
		6-10	Clay, yellow-brown; interlaminated with dark grey at 8-10 cm
		10-25	Muddy sand, grey
44	248	0-4	Sandy mud, yellow-brown; interlaminated with underlying unit at 2-4 cm
		4-32	Muddy sand, grey; 1 cm-thick, dark brown layer with carbonaceous material at 5 cm
45	306	0-27	Clay mud, brown; occasional iron-oxide mottling
		27-43	Sandy mud, medium grey
46	212	0-15	Clay mud, brown; grades downward to grey-brown; abundant calcareous foraminifera
		15-20	Clay mud, light red-brown; contains 3-4 mm-thick layers of very fine sand; base sharp
		20-30	Sandy mud, grey; grades downward to clean quartz sand at 29-30 cm
47	272	0-49 cm	Clay mud, yellow-brown; approximately 5 per cent sand grains; interbedded with 1 cm-thick, light grey layers at 39-49 cm
48	348	0-16	Clay mud, yellow-brown
		16-28	Sandy mud, yellow-brown
49	162	0-7	Sandy mud, yellow-brown; rare .25-0.5 mm, carbonaceous fragments
		7-16	Sandy mud, light grey
50	187	0-2	Clay mud, yellow-brown, base sharp
		2-15	Clay mud, black
		15-27	Muddy sand, black; flat-bedded, 1/2-1 mm-thick layers; 1/2 cm-thick layers clean, white sand at 20.22 cm
51	153	0-7	Muddy sand, yellow-brown; 0.5-1 cm-thick, lensoidal sand layers at 5-7 cm

Core No.	Depth of Water (Metres)		Description (Top to Bottom)
52	168	0-12 cm	Clay mud, yellow-brown; 2 to 5 mm-thick layers of pink-brown clay mud at 6-12 cm; 5 mm-thick layer blue-grey clay mud at 6 cm
		12-22	Clay mud, pink-brown; 1 cm-thick layer of light grey, grading downward to dark grey, clay mud at 12 cm
		22-39	Clay mud, grey; pods of fine sandy mud at 35-39 cm
53	324	0-7	Clay mud, brown, base transitional
		7-32	Clay mud, red-brown; interbedded at base with underlying unit
		32-36	Sandy mud, grey-brown
		36-45	Sandy mud, light grey; thin-bedded; contains scattered pebbles of grey-green sandstone as large as 2 cm
54	356	0-4 cm	Clay, yellow-brown
		4-12	Sandy mud, yellow-brown
55	469	0-7	Clay, yellow-brown; rare worm burrows
56	242	0-17	Sand, yellow-brown
57	296		Sand, yellow-brown
58	382	0-8	Clay, yellow-brown; rare, 0.5-1 mm, red rock fragments
		8-32	Clay, grey; frequent .25-.50 mm grey shale fragments; massive
		32-43	Sandy clay, grey-brown; approximately 5 per cent .25-.50 mm, red rock fragments; 2 cm-thick bed clean sand at 32 cm
59	437	0-5 cm	Clay mud, yellow-brown, with calcareous foraminifera
		5-15 cm	Clay mud, grey
60	411	0-14 cm	Clay mud, yellow-brown, interlaminated with grey mud at 7-14 cm; 4 per cent fine to medium sand
		14-31 cm	Clay, grey
		31-64 cm	Sandy mud, grey

Core No.	Depth of Water (Metres)		Description (Top to Bottom)
61	338	0-6 cm	Clay mud, yellow-brown
62	151	0-23 cm	Sandy mud, yellow-brown, very abundant calcareous foraminifera; contains 2 mm-thick zones of medium sand; few broken pelecypod valves; base sharp
		23-24 cm	Sandy mud, orange-brown, fine to very fine; heavily stained by iron oxide; limonitic plant fibre casts
		24-53 cm	Sandy mud, grey, frequent light grey sandstone fine pebbles; abundant pelecypod and calcareous worm burrow material at 24-29 cm
63	377	0-16 cm	Clay mud, yellow-brown, interlaminated with 2 mm-thick grey mud layers at 3-16 cm; occasional aggregates grey mud, 1/2-1 mm diameter
		16-22 cm	Clay mud, grey
		22-54 cm	Clay, grey, no apparent bedding; 1 cm-thick bed of quartzose sand, very fine, slightly muddy, at 35 cm from top
		54-42 cm	Clay mud, grey, abundant coarse-grain to granule size, grey, fissile clay fragments throughout; occasional yellow-brown clay fragments; total clay fragments about 1 per cent of matrix
64	274	0-12 cm	Sandy mud, yellow-brown, abundant calcareous foraminifera; interlaminated with dark grey mud in layers 1-2 cm thick in lower half
		12-18 cm	Muddy sand, fine, grey, no apparent bedding
65	316	0-6 cm	Clay mud, yellow-brown
		6-7 cm	Sand, fine, orange-brown; iron oxide-stained
		7-20 cm	Clay mud, brown, slightly dark grey mottling at 7-12 cm; base sharp
		20-111 cm	Clay mud, light grey, very finely, flatly, laminated, throughout; laminae 1 mm-5 mm thick; graded bedding, from clay to coarse silt, throughout; colour banding, dark grey or purplish to very light

Core No.	Depth of Water (Metres)		Description (Top to Bottom)
65 (cont'd)	316	20-111 cm	grey-white, overall; dark coloured layers generally finest, grading upward to light coloured and coarser layers; dark layers sharp at base; colour bands 1/4-1/2 cm thick
66	297	0-12 cm	Clay mud, yellow-brown, abundant calcareous foraminifera; calcareous worm tube, plant debris at surface
		12-15 cm	Sandy mud, yellow-brown; frequent fine pebbles grey sandstone
67	374	0-19 cm	Clay, yellow-brown, abundant calcareous foraminifera; irregular, light grey mottling; brown colour banding at 9-19 cm; base sharp
		19-59 cm	Clay mud, grey, no apparent bedding sand fine to medium, quartzose; 1/2 cm diameter, angular gypsum fragment at 49 cm; light brown sandy mud layer at 53 cm
68	352	0-15 cm	Clay mud, yellow-brown, slight dark grey mottling in lower 7 cm; few calcareous foraminifera; base sharp
		15-16 cm	Sand, orange-brown, fine to very fine; closely packed; base sharp
		16-47 cm	Clay mud, grey, no apparent bedding; hematite-red, fissile claystone fragments, 1/2-1 cm, at 16-18 cm; grey claystone fine pebbles throughout, rare; trace grey sandstone fine pebbles
69	298	0-15 cm	Clay mud, yellow-brown, no apparent structure; abundant calcareous foraminifera
		15-17 cm	Muddy sand, yellow-brown, medium to coarse, fairly well sorted, subangular to subround; quartzose
70	279	0-13 cm	Clay mud, yellow-brown, well-defined grey laminae at 6-13 cm, structureless at top; few calcareous foraminifera
		13-88 cm	Clay, dark grey, interlaminated and thinly interbedded with beds of slightly lighter colour throughout; bedding flat; bases of

Core No.	Depth of Water (Metres)		Description (Top to Bottom)
70 (cont'd)	279	13-88 cm	dark layers sharp, grade upward to lighter beds; no visible textural differences; laminae 1 mm-5 mm beds 5 mm-2 cm thick; base sharp
		88-141 cm	Sandy mud, grey; no apparent bedding few light brown pebbles throughout
71	452	0-27 cm	Clay, yellow-brown, structureless at 0-12 cm; 12-27 cm mottled and streaked with grey mud spots; some slightly lighter coloured mottling, probably burrow fillings
		27-44 cm	Clay mud, dark grey, thin-bedded, flat; some dark and light colour banding, at 35 cm; slight fine and very fine sand content increases to 10 per cent at base; base transitional
		44-66 cm	Muddy sand, brown, fine and very fine, frequent fine pebbles; well imbricated but vertically undifferentiated; base sharp
		66-101 cm	Sandy mud, dark grey, slightly gravelly; 15 per cent dark grey shale coarse grains and granules; no apparent bedding
72	336	0-71 cm	Clay mud, yellow-brown, structureless in upper 10 cm; interlaminated with dark grey mud at 10-17 cm; base sharp
		17-39 cm	Sandy clay, grey, 30 per cent quartzose, fine sand; massive
73	186	0-10 cm	Mud, grey-brown, few laminae of dark grey mud
		10-13 cm	Mud, orange-brown, iron oxide-stained, compact; very thin, flat colour banding by slightly lighter laminae
		13-50 cm	Mud, grey and dark grey, no apparent layering; mottled irregularly; base sharp
		50-90 cm	Mud, grey, becomes slightly sandy at base; sand quartz, fine-very fine; no apparent bedding; base transitional
		90-125 cm	Muddy sand, grey, coarse; quartz; subangular to subround; well packed; no apparent bedding; imbricated; base transitional
		125-133 cm	Sandy mud, grey, very thinly, flat, bedded; compact

Core No.	Depth of Water (Metres)		Description (Top to Bottom)
73 (cont'd)	186	133-144 cm	Muddy sand, grey, medium, fairly well sorted; frequent fine pebbles of grey clay shale
74	313	0-16 cm	Clay mud, yellow-brown, faint dark grey mottling
		16-21 cm	Clay mud, yellow-brown and grey, interlaminated, flat; laminae 3 mm thick; no apparent textural difference between colours
		21-162 cm	Clay, grey, composed of dark grey and light grey layers in cyclical sequence; dark layers grade upward to light layers, which are sharply truncated by dark layers; cycles 2 mm to 2 cm thick; no apparent textural variation
75	533	0-19 cm	Clay, yellow-brown; irregular, grey mottling at 10-19 cm
		19-60 cm	Clay, grey, finely laminated
		60-87 cm	Sandy mud, grey; massive
		87-111 cm	Clay, grey, massive
76	398	0-19 cm	Clay, yellow-brown; 5 per cent fine sand; interlaminated with dark grey mud at 16-19 cm; iron oxide staining in 2 laminae
		19-107 cm	Clay mud, grey, composed of dark grey and light grey layers in cyclical sequence; dark layers grade upward to light layers, which are sharply truncated by dark layers; dark layers very slightly coarser
77	494	0-30 cm	Clay mud and clay yellow-brown, 10 per cent fine sand at 0-10 cm; interlaminated with grey and iron oxide-stained layers at 14-30 cm; base sharp
		30-101 cm	Clay mud, grey, cyclically layered, layers 1/2 mm-1 cm thick; dark layers grade upward to light layers, which are sharply overlain by dark layers
		101-118 cm	Muddy sand, grey, few fine pebbles, randomly distributed; sand fine-very fine, round-subround occasional granules grey clay shale

Core No.	Depth of Water (Metres)		Description (Top to Bottom)
78	395	0-11 cm	Clay mud, yellow-brown, no apparent bedding
		11-41 cm	Clay mud; light brown, mottled with grey mud; interbedded with dark grey mud containing granules and fine pebbles of grey shale; 1 cm thick grey layer at 17 cm; 4 cm thick layer at 26 cm; very fine, flat laminated structures visible throughout unit; base transitional
		41-85 cm	Clay, dark grey, finely interlaminated with light brown mud; cyclical sequence of dark layers grading upward to light layers, which are overlain sharply by dark layers; 1/2 cm thick layer of very fine, clean white sand at 71 cm
79	188	0-7 cm	Sandy mud, yellow-brown; frequent blebs of iron oxide staining; base transitional
		7-95 cm	Sandy mud, dark grey, slightly gravelly; dry and compact; no apparent bedding; shale, limestone, and metamorphic rock granules throughout; frequent fine pebbles of same composition
80	416	0-25 cm	Clay, yellow-brown, uniform, no apparent bedding; very faint grey mottling, as of disrupted bedding, at 23-25 cm
		25-30 cm	Clay, grey-brown; grey mottling at 25-29 cm becomes irregular bedding in lower part; laminae 2-3 mm thick; laminae are alternately grey and brown but do not grade into one another; unit is transitional between one above and one below
		30-60 cm	Clay, light grey, well defined laminae in cyclical sequence of darker layers grading upward to lighter layers, which are sharply overlain by darker layers; layers at base thinner and more closely spaced (1-2 mm) than at top (3-4 mm)
		60-73 cm	Muddy sand, grey, quartzose; fine sand fraction well sorted; very fine sandy mud at 60-65 cm

APPENDIX B

Textural characteristics of sediment samples

Core No.	Sample Interval (cm from top)	Per Cent By Weight Sand	Silt	Clay	ϕMd	ϕp16	ϕp84	∂G*
1	0-4	9	19	73	9.8	4.8		
2	0-4	1	17	82	10.2	7.4		
3	0-4	2	23	75	12.0	6.9		
3	40-44	10	16	74	9.5	6.1		
4	0-4	7	15	78	10.0	6.8		
4	9-13	67	11	22	2.8	2.0	9.0	3.5
5	0-4	2	16	82	10.2	7.4		
5	24-28	35	27	38	5.8	3.2		
5	40-44	24	26	50	7.6	3.4		
6	0-4	2	17	81	10.2	7.3		
6	34-38	20	25	55	8.4	7.4		
7	0-4	3	13	84	10.2	7.4		
7	26-30	22	28	50	7.6	3.5		
8	0-4	3	21	76	9.8	6.9		
8	45-49	13	17	70	7.0	3.9	10.9	3.5
8	55-59	3	57	40	7.0	5.3	10.8	2.75
9	0-4	3	21	76	10.0	6.8		
9	30-34	2	17	81	10.4	7.5		
9	64-68	0	18	82	10.2	7.5		
10	0-4	3	18	79	10.0	7.1		
10	17-20	2	21	77	10.0	6.8		
10	30-34	2	13	85	10.2	7.6		
11	0-4	3	24	73	9.8	6.4		
11	30-34	0	18	82	10.2	7.4		
11	63-66	2	28	70	9.3	6.7		
11	69-72	50	22	28	4.3	2.0	10.4	4.2
12	0-4	0	15	85	10.4	7.8		
12	30-34	20	24	46	8.4	2.9		
13	0-4	0	15	85	10.4	7.8		
13	19-23	22	30	48	7.4	2.6		
14	0-7	2	18	80	10.0	7.3		
15	0-4	11	34	55	8.2	4.7		
16	0-4	3	15	82	10.2	7.3		
17	0-4	2	21	77	9.8	6.9		
18	0-4	2	21	77	9.8	6.9		
18	40-44	0	26	74	9.8	6.5		
18	70-73	48	28	32	4.6	2.2		

*Graphic Standard Deviation

Core No.	Sample Interval (cm from top)	Per Cent By Weight Sand	Silt	Clay	ϕMd	ϕp16	ϕp84	∂G
20	0-4	6	26	68	10.0	5.5		
20	22-26				6.1	2.2		
21	0-4	7	18	75	9.3	6.5		
21	22-26	0	22	78	10.1	7.0		
22	0-4	4	14	82	10.2	7.4		
22	12-16	24	42	36	5.8	7.3		
23	0-4	53	12	35	3.9	2.4		
23	25-29	50	22	28	4.3	2.0		
24	0-4	18	33	49	7.5	4.0		
24	26-30	30	23	47	7.2	5.8		
25	0-4	15	23	62	9.0	3.3		
26	0-4	32	18	50	7.6	2.0		
26	30-33	33	28	39	5.7	2.2		
26	38-42	5	34	61	9.2	5.1		
27	0-4	7	14	79	9.8	7.1		
28	0-4	53	17	30	4.0	2.8	10.4	3.8
29	0-4	47	20	33	8.0	5.8		
29	10-14	39	24	37	8.8	2.5		
30	0-4	40	25	35	5.1	2.6		
31	0-4	3	17	80	10.0	7.2		
31	19-23	1	27	72	9.3	6.6		
32	0-4	4	23	73	9.6	6.4		
32	10-14	28	26	46	7.2	2.8		
33	0-4	2	23	75	9.8	6.2		
33	12-16	44	16	40	8.3	2.5		
34	0-4	7	20	73	9.6	6.3		
34	19-23	57	16	27	3.7	2.3		
35	0-4	40	25	35	5.0	2.4		
36	0-4	2	36	62	9.0	5.7		
37	0-4	7	20	73	9.3	9.7		
37	8-13	53	20	27	3.9	2.4	10.2	4.0
38	0-4	10	28	62	8.6	8.3		
38	22-26	48	20	32	4.6	2.2		
39	0-4	3	30	67	8.8	5.8		
39	40-44	0	23	77	9.8	6.9		
40	0-4	42	18	40	6.0	2.5	10.4	2.5
41	0-4	3	47	50	7.6	5.5		
41	13-17	11	19	70	9.8	6.4		
42	0-4	3	25	72	9.3	6.5		
42	25-29	24	32	44	7.4	3.4		
42	39-42	36	27	37	5.6	2.5		
43	0-4	4	22	74	9.5	6.6		
43	15-19	50	22	28	4.3	3.0		
44	0-4	42	22	36	4.8	2.2		
44	26-30	60	13	27	3.3	1.8		

Core No.	Sample Interval (cm from top)	Per Cent By Weight Sand	Silt	Clay	ϕMd	ϕp16	ϕp84	∂ G
45	0-4	3	42	55	9.0	5.5		
45	25-29	37	20	43	6.1	2.7		
46	0-4	2	23	75	9.5	6.8		
46	13-17	4	27	69	9.6	5.8		
46	24-28	35	30	35	5.8	2.7		
47	0-4	7	38	55	8.3	4.8		
47	26-30	0	30	70	9.5	6.3		
48	0-4	3	19	78	9.7	7.4		
48	22-26	42	28	30	4.8	3.0		
49	0-4	46	22	32	4.8	3.0		
50	0-4	13	20	67	9.5	4.6		
50	18-22	53	25	22	4.0	2.4	9.0	3.2
51	Snapper Sample	67	15	18	2.9	1.7	8.4	3.35
52	0-4	9	21	70	9.7	5.1		
52	18-22	2	16	82	10.2	7.1		
53	0-4	2	21	77	9.8	6.9		
53	20-24	0	26	74	10.0	6.3		
53	41-45	40	25	35	5.5	2.7		
54	0-4	10	27	63	9.2	4.8		
55	0-4	3	27	70	9.5	5.8		
56	0-4	76	11	13				
57	Snapper Sample	77	13	10	3.6	3.0	5.6	1.3
58	0-5	3	28	69	9.5	6.3		
58	33-37	47	19	34	8.4	2.5		
59	0-4	22	29	49	7.7	3.7		
60	0-4	5	23	72	9.5	6.3		
60	20-24	2	17	81	10.2	7.5		
60	36-40	25	22	53	8.1	3.6		
61	0-4	21	23	56	8.1	3.6		
62	0-5	40	25	35	5.2	3.0		
62	35-38	36	20	44	6.4	3.0		
63	0-4	10	18	72	9.8	6.3		
63	16-20	25	32	33	5.3	4.1		
63	27-31	0	15	85	10.4	7.7		
63	49-53	4	14	82	10.1	7.3		
63	86-90	18	25	57	8.5	7.3		
64	0-4	31	30	39	5.8	3.5		
65	0-5	7	30	63	9.5	5.4		
65	11-15	7	29	64	8.6	5.5		
66	0-4	8	27	65	9.2	5.9		
67	0-4	5	18	77	10.2	6.8		
67	40-44	20	25	55	8.4	7.4		
68	0-5	5	18	77	10.0	6.8		
68	15-19	17	20	63	8.8	4.1		
69	0-4	10	23	67	9.5	5.8		

Core No.	Sample Interval (cm from top)	Per Cent By Weight Sand	Silt	Clay	ϕ Md	ϕp16	ϕp84	∂G
70	0-4	5	20	75	10.0	6.7		
70	45-49	2	8	90	10.6	7.8		
70	120-124	42	20	38	5.6	2.9		
71	0-4	12	11	77	10.0	6.4		
71	40-44	5	30	65	9.8	5.9		
71	55-59	67	13	20	6.4	5.2	10.0	2.4
71	85-89	33	22	45	7.1	2.9		
72	0-4	5	19	76	9.8	6.3		
72	34-38	28	21	51	7.8	2.7		
74	0-4	10	17	73	10.0	5.9		
74	55-60	2	16	82	10.0	7.4		
75	0-5	3	13	84	10.0	7.4		
75	77-81	32	20	48	7.4	2.7		
76	0-4	5	15	80	10.0	7.3		
76	46-50	32	20	48	10.0	6.9		
77	0-4	2	21	77	10.0	7.2		
77	26-30	2	18	80	10.0	7.2		
77	110-114	43	22	35	5.1	5.9	10+	
78	0-4	22	23	55	8.4	4.0		
78	28-32	10	22	68	9.5	5.1		
78	65-69	9	18	73	10.0	5.9		
78	98-102	3	20	77	10.0	6.8		
79	0-5	47	18	35	4.6	2.6	10.3	3.55
79	51-57	48	20	32	4.5	2.6		
80	0-4	10	18	78	9.6	5.8		
80	53-57	0	21	79	10.8	7.0		
80	70-74	63	12	25	3.5	2.1	10.6	4.25

STREAM MOUTH AND FORESHORE SAMPLES

For Locations, See Fig. 14

Sample No.	Per Cent By Weight						
Stream Mouth Samples	Sand	Silt	Clay	ϕ Md	ϕ p16	ϕ p84	∂g
A-1	100	0	0	1.7	1.2	2.5	0.65
B-1	100	0	0	1.5	0.6	2.4	.90
C-1	100	0	0	1.7	0.9	2.8	.95
* D-1	60	22	0	1.2	-0.5	4.3	2.4
E-1	100	0	0	1.4	0.5	2.0	.75
F-1	100	0	0	1.8	1.1	2.6	.75
* G-1	90	0	0	1.6	0.5	2.5	1.00
* H-1	65	0	0	1.2	-2.0	2.5	2.25
* J-1	93	0	0	1.5	0.5	2.3	.90
K-1	100	0	0	2.4	1.3	3.2	.95
* L-1	85	10	0	2.2	0.2	3.9	1.35
*M-1	95	0	0	1.5	0.5	2.5	1.0
N-1	100	0	0	2.3	1.5	2.8	1.15
P-1	95	5	0	2.4	1.3	3.2	1.95
* Q-1	90	0	0	1.4	0.3	2.5	1.1
R-1	93	7	0	1.9	1.1	3.1	1.0
T-1	100	0	0	1.8	1.0	2.5	1.25
Foreshore Samples							
0-1	87	13	0	2.3	1.4	3.1	0.85
0-8	83	10	7	2.7	1.5	4.6	1.55
0-12	90	7	3	2.7	1.3	3.9	1.30
* 0-13	85	5	0	2.0	0.5	3.0	1.25

APPENDIX C

Compositions of sand fractions lighter than bromoform

All sand is quartz except as indicated in this appendix

Core No.	Sample Interval (cm)	% Grey Mudstone	% Brown Mudstone	% Pyritic Mudstone	% Rusty Quartz	% Sandstone	% Feldspar	Remarks
2	0-4					1 (Red)	6	1% Shell
3	0-4					1 (Red)		TR "
3	40-44					TR (Grey)	1	
4	0-4					TR (Grey		
5	0-4					2 (Red)		1% "
5	24-28	2				TR (Glauconitic)		
5	40-44		1				3	
6	0-4		1					10% "
6	34-38		3					
7	0-4		3		30	TR		
7	26-30						TR	
8	0-4		1					
8	45-49							2% Wood Fragments
8	55-59	20						1% Basalt; TR Metamorphics
9	0-4	3						
10	0-4	TR				20		
10	17-20	15				3 (Brown)		TR Schist
10	30-34		10					
11	0-4			3			5	
11	30-34			15				
12	0-4		1		40			
12	30-34					TR	1	

13	0-4		2				8	
14	0-7	3						
15	0-4		1				TR	
20	0-4			1				
20	22-26			20				
21	0-4			TR				
21	22-26							Clean Quartz
22	0-4							" "
22	12-16		2					
23	0-4			1		1 (Glauconitic)		
23	25-29			3				
24	0-4	1	1		3			
24	26-30	8				2 (Brown)	1	
25	0-4	10						
26	0-4			1		1 (Rusty)		
26	30-33		3				5	1% Basalt
26	38-42		1				4	
27	0-4	1						1% Basalt
28	0-4	1	1					
28	12-16		15				10	
29	0-4		3					
29	10-14					2 (Grey)		
						1 (Glauconitic)		1% Basalt
30	0-4			1	3			1% Basalt; 1% Shell
31	0-4			1				
31	19-23			6				
32	0-4	1						2% Shell
32	10-14		1			TR (Glauconitic)	10	
33	0-4		1					
33	12-16			1				
34	0-4			2	5		TR	
34	19-23							TR Polished Basalt
35	0-4		30					
36	0-4	5	5					

Core No.	Sample Interval (cm)	% Grey Mudstone	% Brown Mudstone	% Pyritic Mudstone	% Rusty Quartz	% Sandstone	% Feldspar	Remarks
37	0-4		TR		30			
37	8-13					1 (Brown)		
38	0-4							TR Basalt
38	22-26					TR (Brown)		
39	0-4			1	30			
39	40-44					TR (Red)		
40	0-4		TR				10	
41	0-4		30					
41	13-17	1						1% Basalt
42	0-4					3 (Brown)	12	
42	25-29		3					
43	0-4		2					
43	15-19		3					
44	0-4					TR (Brown)	2	
44	26-30						1	Clean Quartz
45	0-4	5	15					
45	25-29							1% Basalt
46	0-4	15					5	
46	13-17	15 (Black)					8	
48	0-4			1	25		3	
48	22-26	8						
49	0-4					2 (Brown)		
50	0-4	2					3	
51	Snapper Sample							TR Basalt
52	0-4					3 (Brown)		
52	18-22					TR (Grey)		1% Gypsum
53	0-4				20		5	
53	20-24		2					

53	41-45		3		TR (Grey)	15	
54	0-4		TR				
55	0-4			2		1	
56	0-4	TR	TR			7	
58	0-4	3				13	
60	0-4						3% Shells & Spicules
60	20-24	3					
61	0-4	TR					2% Shell Fragments
63	0-4	2			TR (Red)		
65	0-4	3					
67	0-4					5	5% Shell Fragments
68	0-5				2 (Grey)		
70	0-4						Clean Quartz
70	45-49						" "
71	0-4						" "
71	40-44		TR				
71	55-59		5				
71	85-89						" "
72	0-4			10			
72	34-38						" "
74	0-4			20			1% Shell Fragments
74	55-60						Clean Quartz
75	0-4						1% Shell Fragments
76	0-4						" " "
76	46-50				TR (Grey)		
77	0-4		TR				
77	26-30		10				
77	110-114	2					
78	0-4				TR (Grey)		
78	28-32	1					
79	0-4				1 (Grey)		
79	51-57						Clean Quartz
80	0-4			50			TR Shell Fragments
80	53-57				1 (Grey)		

APPENDIX D

Compositions of sand fractions heavier than bromoform

(Figures indicate abundances of mineral species relative to total heavy mineral fraction, given to nearest whole per cent. "X" indicates abundances of less than 1 per cent.)

CORE SAMPLES

Core No.	Interval (cm)	ILM/MAG (UNOX.)	Pyrite	Ox Opaques	Garnet	Tourmaline	Kyanite	Zircon	Rutile	Staurolite	Hornblende	Apatite	Diopside	Augite	Olivine	Epidote	Calcite	
1	0-4	14		54	8			3										8% Siderite
2	0-4	36		36	10			3	3									7% Sphene
3	0-4	29		27	8	7		4	3		8							4% "
3	40-44	1	14	78	2	X			X									
4	0-4	24		69	4	X	X		2									
4	9-13	35	10	21	6	8	7		2	1		1						4% Monazite
5	0-4	17		30	4	23	1				4							
5	24-28	61		13	6	6	X	2	1	X		X						
5	40-44		74	10	7	1		2	1									
6	0-4	23		47	5	4	2		3		3		7		3			
6	34-38	67		10	10		1	X	3	2	1	4						
7	0-4	41		35	4	2	X	1	3	1	1	2		1				5% Chlorite; 3% Siderite
7	26-30		75	5	7	7				1								
8	0-4	13		60	4	2	X	1	2		1	1		2				

8	45-49	20		54	10	3	1	2	X	X						
9	0-4	73		10	2			1	4				1	3		
12	0-4	5		90	2		X	X	X				X	X		
12	30-34	75		9	3	1		2				3				
13	0-4	18		27	7	7	X		8		X	X	X		4	4
13	19-23	63		9	10	1	X	1	1	1	X	X	1		2	2
14	0-7			56	5	5	X	2	3	1	X	2		X	2	1
15	0-4	4		88	3	1							1		2	
16	0-4	23		51		8										
17	0-4	11		78	1	3		2	2			1	X			X
18	0-4	15		62	5	2			X		2				4	X
18	40-44	Few grains of black, rounded opaque minerals.														
18	70-73	61		11	6	2		2								
19	Snapper Sample		58	19	11	2	X	X	X	2					X	X
20	0-4		73	22		X			X							
20	22-26	68		26	3				X	2			X			
21	0-4	30		43	3	4	X	1	5	X	X	1	5	X	1	2
22	12-16		98	X	1						X					
23	0-4		67	23	4	1	X	X	1	X		X			X	
23	25-29	62		22	5	1		4	3	1						
24	0-4	18		70	4	2			2	4						
24	26-30	17	17	59	3	X			2							
25	0-4	8		90	1			X		X						
26	0-4	14		65	7	3		1	4		X	X	1	X	2	X
26	30-33	50		47	2											
26	38-42	34		48	5	3		X	X		3	X	X			
27	0-4		95	3		X		X	X				X			X
28	0-4	18		69	7	2	X	X	1	X		X	X		X	
28	12-16	23		50	14	3	2	5		2		X			X	
29	0-4	4		94	X							X	X			
29	10-14	71		14	3	6		2	2			2				
30	0-4	15		73	2	4		1	1				X		X	
31	0-4	24		68	3	X		X	1		X			X	1	

Core No.	Interval (cm)	ILM/MAG (UNOX.)	Pyrite	Ox Opaques	Garnet	Tourmaline	Kyanite	Zircon	Rutile	Staurolite	Hornblende	Apatite	Diopside	Augite	Olivine	Epidote	Calcite
31	19-23	61		37	1												
32	0-4	28		47	3	2	1	2	9		X	X			2	2	
32	10-14	18		65	6	X		3	1	1	1	X			X	X	
33	0-4	24		51	6			3					6		6		
33	12-16	54		26	8	4	X	2	1	X		1	X		X		
34	0-4	21		59	11	3	X	X				X	2		X		
34	19-23	45		22	19	3	3	2	X	3	X		X		X	X	
35	0-4	32		51	8	X	2	3		X	X	X	X			X	
37	0-4	36		34	13	4	5		X		3					X	
37	8-13	19		40	26	3	X	1	2	2			X			X	
38	0-4	25		56	6	2	1	3	1	X	3	X			1	X	
38	22-26	45		23	17	2	4	2	X	3	2	X				X	
39	0-4	29		41	7	1		4	X	4	X	X			X		
39	40-44	96		X	2												
40	0-4	38		33	9	1	3	X	2	1		X	1		3	5	
41	0-4	44		40	4	2		2	2								
41	13-17		70	21	4	1		1			X		1	X	1		
42	0-4	35		44	5	5	X	2	X	X		X			3		
42	25-29	38		35	9	5		7	X	X	X	X					
42	39-42	2	63	28	2	2											
43	0-4	24		35	14	5	2	6	2	4	X	3			X		
43	15-19	2	74	16	3	4		2	X								
44	0-4	40		17	24	4	4	2	2	3	X	X	X		1	X	
44	26-30	54		4	22	2	5	2	2	4	X	1	X		X		

45	0-4	18		71	1	2	3						1			1	
45	25-29	38		50	7	1	1		X				X			X	
46	0-4	22		62	4	5		X		X			X	X			
46	13-17	13		54	12	7		9	X	X		3					
47	0-4	32		45	4	3	X	3	2	X	2	3		X	2	2	
48	0-4	19		34	17	6		14	3		4	X		X	X	X	
48	22-26	X	76	18	X	3		1	1			X					
49	0-4	8		86	3	1	X		X	X			X				
50	0-4	51		16	11	4	1	3	1	2	X	X	X		2	2	
50	18-22	27		45	15	X	6	1	X	3			2				
51	Snapper Sample	23		7	41	4	9	1	6	6							
52	0-4	13		56	2	4			1	X	X	1					20% Chlorite
52	18-22	43		39	4	6	X	X	X	X	X	3					
53	0-4	26		45	6	3	X	6	X		6	4	X		X		
53	20-24	34		47	6	6	5	X	X		X	X					
54	41-45	13		74	7	3						2	X				
55	0-4	11		59	4	7	2	4	4		2	3	X	X			
56	0-4	21	6	31	24	9	X	X		5	X			X	X		
57	Snapper Sample	34	15	2	7	17		15	4	3			X				
58	0-5	25		35	8	4	X	10	X	2	4*	2	3		2		*Blue-green Hornblende
58	33-37	21		58	6	6			2		1*	1					*Blue-green Hornblende
60	0-4	12	15	35	8	5		4	1		7	3			2		
60	36-40	9	58	19	5	3		1			1	1					
61	0-4			98		X									X		
65	0-5	4	1	83	3	3		1				1					
65	11-15	32	11	33	3	8					4						
67	0-4	20	X	25	8	8		2			2	5			2	19	
67	40-44	9	53	21	6	3		2							1	11	
68	15-19	14			5	1					3	X	2	1	1	71	
70	0-4	35	4	18	14	8		5		3		6					4% Enstatite

Core No.	Interval (cm)	ILM/MAG (UNOX.)	Pyrite	Ox Opaques	Garnet	Tourmaline	Kyanite	Zircon	Rutile	Staurolite	Hornblende	Apatite	Diopside	Augite	Olivine	Epidote	Calcite	
70	120-124	31	39	9	10	7		1		2								
71	0-4	30	13		20	15							10					
71	40-44	57	1		8	13		11										
71	55-59	13	36		8	16		7			2	2					12	
71	85-89	6	41		10	6						2					29	
72	0-4	18	1	56	7	5								1			7	
72	34-38	6	44	37	11						2	2					65	
74	0-4	10		14	2	4		1			1			1	1		32	
76	0-4	17	3	27	6	8		2			4	10	X	2			2	
77	0-4	21	X	21	17	10		6	2	2								
77	26-30	12	73	13														
77	110-114	7	23	53	6	7		3	1			5				4	6	2
78	0-4	50		17	7	3		2								2	2	2
78	28-32	12	72		4											2	2	
78	65-69	23	17		5	5				2						6		10
79	0-5			99	X	X												4
79	51-57	23	37		16	7		4				1						
80	0-4	14	X	7	3	5					3	2		1			58	
80	70-74	16	7	11	10	8		6				7					18	13% Biotite

STREAM AND OUTCROP SAMPLES - For Locations see Fig. 14

Sample No.	General Location	ILM/MAG	Ox Opaques	Garnet	Tourmaline	Kyanite	Zircon	Rutile	Staurolite	Hornblende	Apatite	Diopside	Augite	Olivine	Epidote	Sillimanite	
A- 1	Beaufort FM.	26		19	6	20		1	12							6	10% Leucoxene
A- 2	Beaufort FM.	59		9	4	7	11	1	1							2	
A- 3	Beaufort FM.	55		14	3	10	6	2	4							4	
A- 4	Beaufort FM.	59	4	3	3	11	10	6	2							1	
A- 5	Beaufort FM.	42		9	8	20	3	1	11							5	
A- 7	Beaufort FM.	44	5	20	7	10	3	2	7								
F- 6	Stream In Isachsen	43		33	6		9	3	3			1					
F- 9	Outcrop, Isachsen FM.	44		30	6		18	2	1								
G- 4	Outcrop, Isachsen FM.	57		22	4		14	4		X	1						
G- 9	Stream, Isachsen FM.	57		26	2		10	4									
G-10	Outcrop, Isachsen FM.	58	6	23	4		3	2			1	1					
H- 8	Outcrop, Christopher FM.	65			X	4	3	2	2	X						X	5% Basaltic Hornblende
J- 1	Stream, Isachsen FM.	43	3	23	3		20	5	1		X				X		
J- 3	Stream, Isachsen FM.	41	22	22	5		18	X	X								
J- 6	Stream, Isachsen FM.	30	28	26	8		2	2	3			X					
J- 8	Stream, Isachsen FM.	29	42	19	5		X	X	X						X		Abundant, Oxidized Sider
J-10	Stream, Isachsen FM.	37	34	19	X		X	2	2								
M- 2	Stream, Christopher(?) FM.	11	76	6	2	2	1		X	X		X				X	
M- 4	Stream, Christopher(?) FM.	41	48	1	3	3	2	X								X	
M- 5	Outcrop, Christopher(?) FM.	35	46	4	1	2	4		2	1							
M- 6	Stream, Christopher(?) FM.	76	10	3	1	1	7	X							X		
M- 8	Outcrop, Christopher(?) FM.	15	1	9	2	1	3	X	1			2		2			52% Pyrite
N- 1	Stream, S. Lougheed Island	59	21	2	7	5	2	1				2			X	X	
N- 3	Stream, S. Lougheed Island	50	14	3	X	7	5		3	X		4	X	X		X	
N- 5	Stream, S. Lougheed Island	76	8	X	3	2	7	1	X			X				1	
N- 7	Outcrop, S. Lougheed Island	62	6	2	7	1	5	3	2	2		3		2	X	X	
P- 3	Outcrop, Central Lougheed Island	60	25	2	2	2	1	2									TR. Pyrite
Q- 3	Outcrop, S. King Christian Island		98	1	1												
Q- 8	Outcrop, S. King Christian Island	80	12		1	4	1		2								

APPENDIX E

List of foraminiferal species identified from bottom samples

(Identifications By G. Vilks, Bedford Institute of Oceanography)

Adercotryma glomeratum (Brady)
Astrononion gallowayi Loeblich and Tappan
Biloculina discus Egger
Buccella frigida (Cushman)
Buccella sp.
Bulimina exilis Brady
Bulimina sp.
Bulimina sp. A
Cassidella complanata (Egger)
Cassidulina islandica Nørvang
Cassidulina norcrossi Cushman
Cassidulina teretis Tappan
Cassidulinoides sp.
Cibicides lobatulus (Walker and Jacob)
Cibicides sp.
Cribrostomoides crassimargo (Norman)
Cribrostomoides jeffreysi (Williamson)
Cruciloculina ericsoni Loeblich and Tappan
Dentalina frobisherensis Loeblich and Tappan
Dentalina pauperata d'Orbigny
Dentalina sp.
Elphidium bartletti Cushman
Elphidium clavatum Cushman
Elphidium orbiculare (Brady)
Elphidium sp.
Eponides tenera (Brady)
Fissurina marginata (Montagu)
Fissurina semimarginata (Reuss)
Fissurina sp.
Fissurina sp. A
Globigerina pachyderma (Ehrenberg)
Globobulimina sp.
Hyperammina friabilis Brady
Hyperammina sp.
Lagena flatulenta Loeblich and Tappan
Lagena laevis (Montagu)
Lagena lateralis Cushman
?Lagena meridionalis Wiesner
Lagena sp.

Lagena sp. A
Lagenidae, gen. sp. indet.
Miliolinella chukchiensis Loeblich and Tappan
Nonion labradoricum (Dawson)
Nonion zaandamae (van Voorthuysen)
Nummoloculina sp.
Nummoloculina sp. A
Nummoloculina sp. B
Oolina caudigera (Wiesner)
Oolina costata (Williamson)
Oolina cf. O. costata (Williamson)
Oolina hexagona (Williamson)
Oolina melo d'Orbigny
Oolina cf. O. melo d'Orbigny
Parafissurina arctica Green
Parafissurina sp. A
Proteonina atlantica Cushman
Proteonina sp.
Psammosphaera fusca Schulze
?Pyrgo williamsoni (Silvestri)
Quinqueloculina arctica Cushman
Quinqueloculina seminulum (Linné)
Quinqueloculina sp.
Quinqueloculina sp. A
Quinqueloculina sp. B
Recurvoides turbinatus (Brady)
Reophax curtus Cushman
Reophax guttifer Brady
Reophax nodulosus Brady
?Reophax sp.
Robertinoides (?) charlottensis (Cushman)
Saccorhiza ramosa (Brady)
Spirillina vivipara Ehrenberg
Spiroplectammina biformis (Parker and Jones)
Textularia torquata Parker
Triloculina sp. A
Trochammina globigeriniformis (Parker and Jones)
Trochammina nana (Brady)
Trochammina quadriloba Höglund
Trochammina squamata Jones and Parker
Trochamminella atlantica Parker
Valvulineria arctica Green
Virgulina fusiformis (Williamson)